Elliott Bloom
KIPAC-SLAC, Stanford University

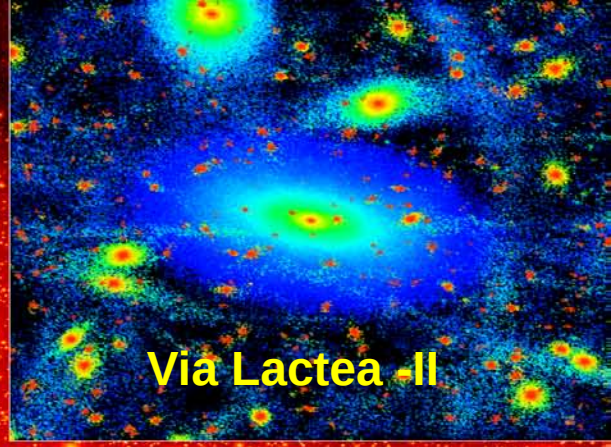

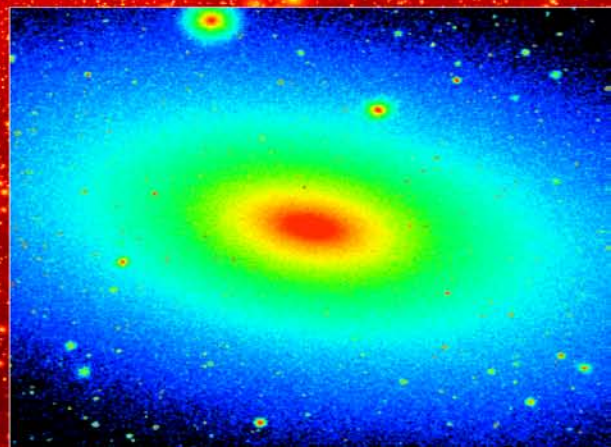

Fermi Lab Colloquium
March 30, 2011

Via Lactea II

What's Coming

- Dark matter candidates
- Overview of the Fermi LAT (Fermi LAT – Collaboration)
- The Milky Way as seen through the eyes of the Fermi-LAT (Fermi LAT Collaboration)
- Fermi Search for Dark Matter Update (Fermi LAT – Collaboration)
  - electrons and positrons
  - extra galactic background
  - Known and unknown dwarf galaxies
  - Gamma line search
  - The search for extra large dimensions (ADD)
- Future with CTA (Stefan Funk)

Particle Dark Matter?

- Most widely accepted assumption so far: dark matter is made out of particles
- What data tell us about dark matter:
  - it interacts very weakly, and at least gravitationally, with ordinary matter
  - it is cold, i.e. non-relativistic
  - it is neutral
  - it is stable (or it is very long-lived)

➡ However no known particles are good candidates for dark matter!

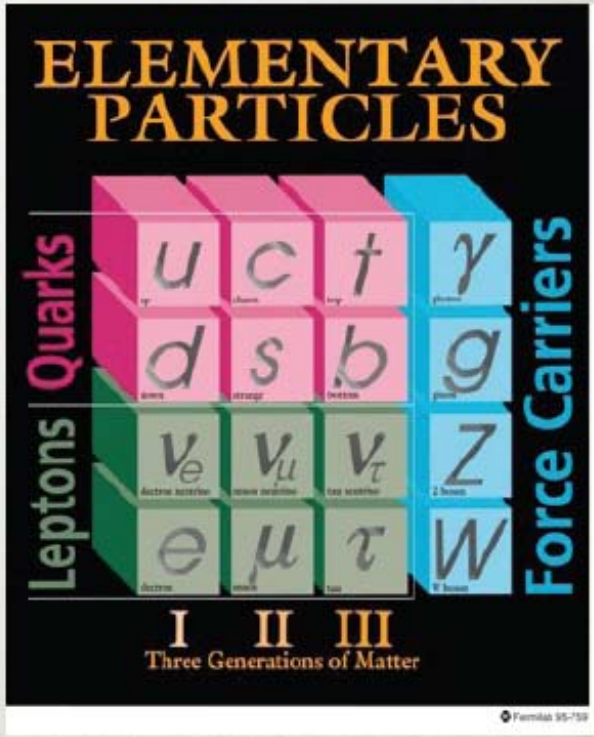

Dark Matter Candidates

- Several beyond the Standard Model of particle physics scenarios have been proposed that naturally predict the existence of new particles that are excellent dark matter candidates

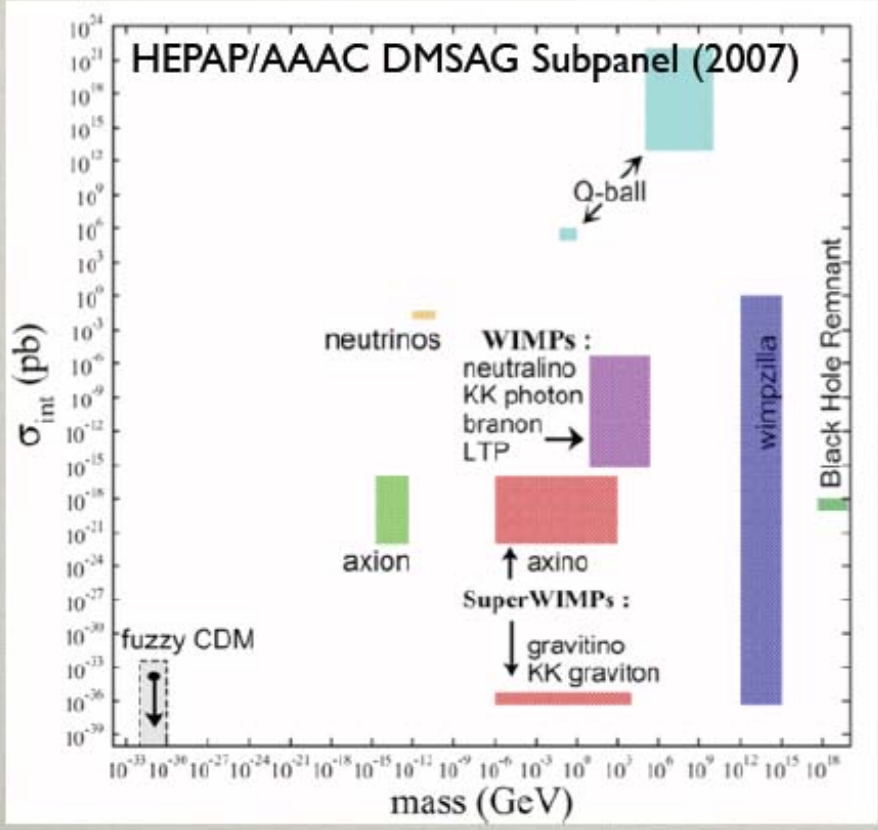

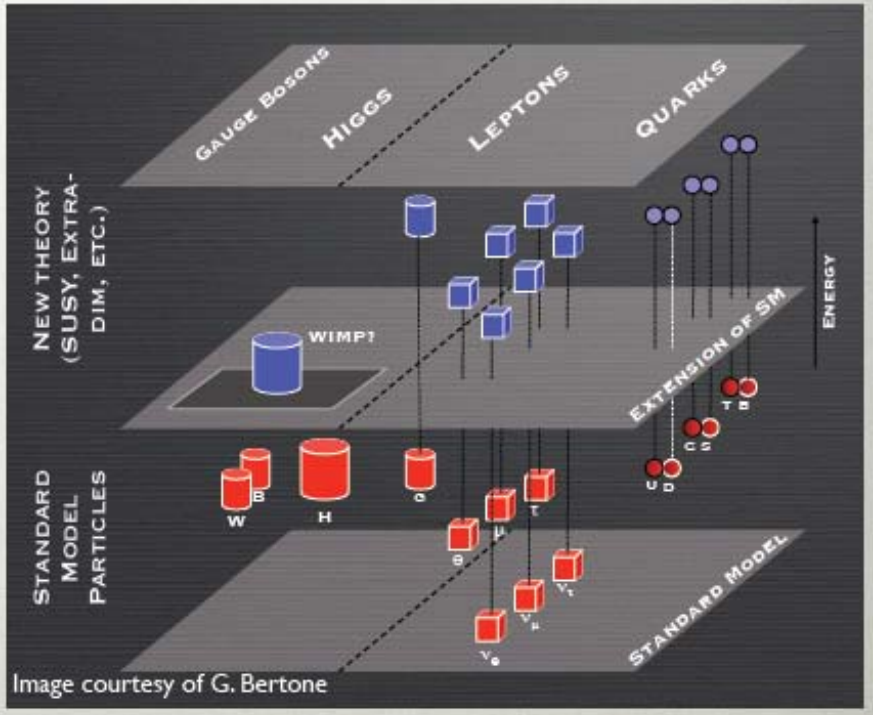

Dark Matter Candidates

- Several beyond the Standard Model of particle physics scenarios have been proposed that naturally predict the existence of new particles that are excellent dark matter candidates

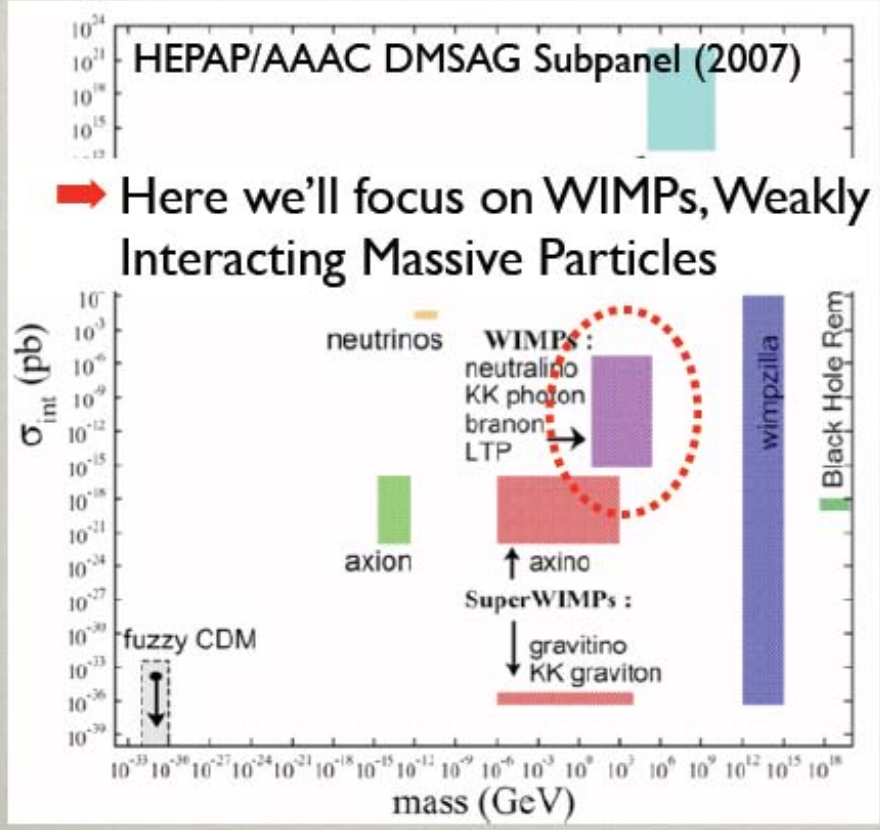

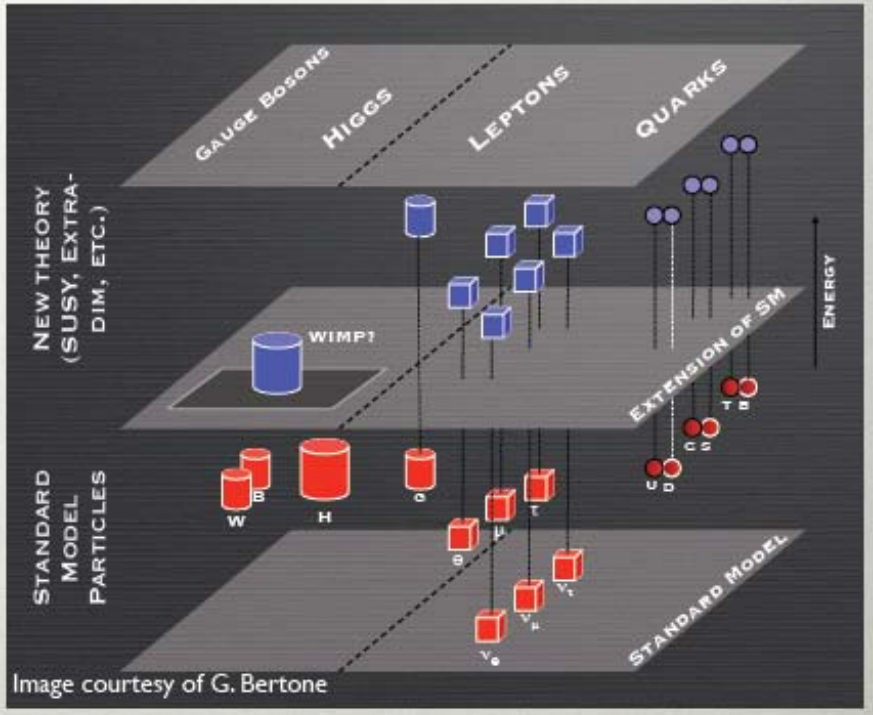

Image courtesy of G. Bertone

WIMP Dark Matter

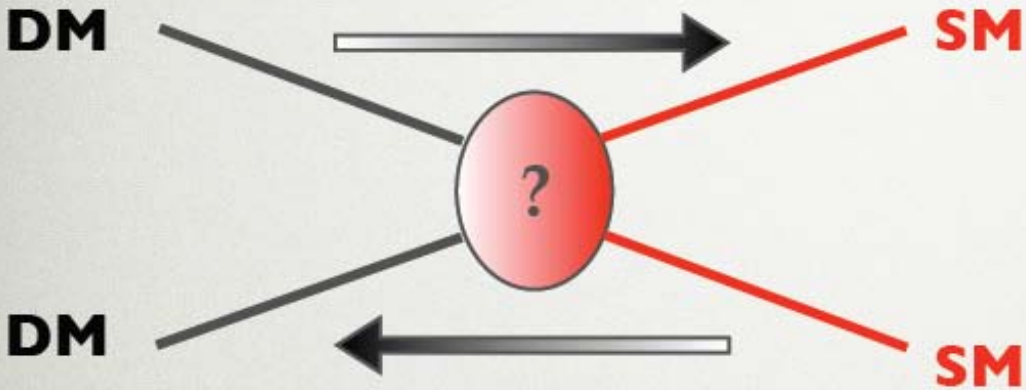

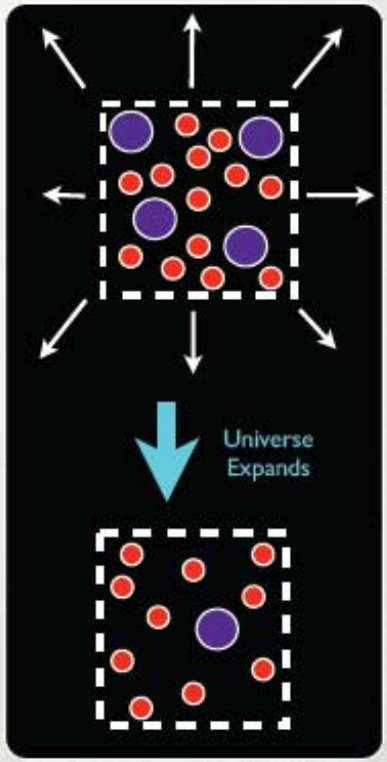

- For weak scale interactions between dark matter and SM particles, a *typical* thermal WIMP has:
  - mass of order **100 GeV**
  - annihilation cross section of order **3×10^{-26} cm^3 s^{-1}**

~ three 100 GeV WIMPs per liter in the room

➡ Many current and planned experiments are sensitive to a broad range of WIMP models

Dark Matter WIMP Searches

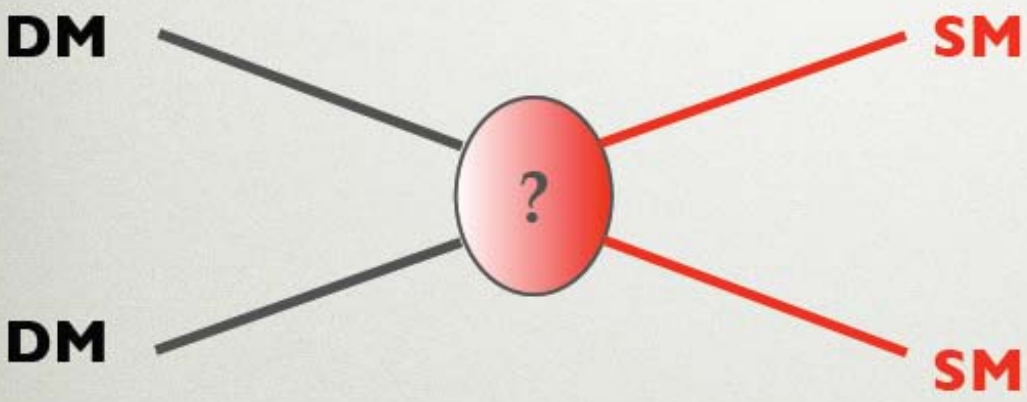

Dark Matter WIMP Searches

COLLIDER SEARCHES

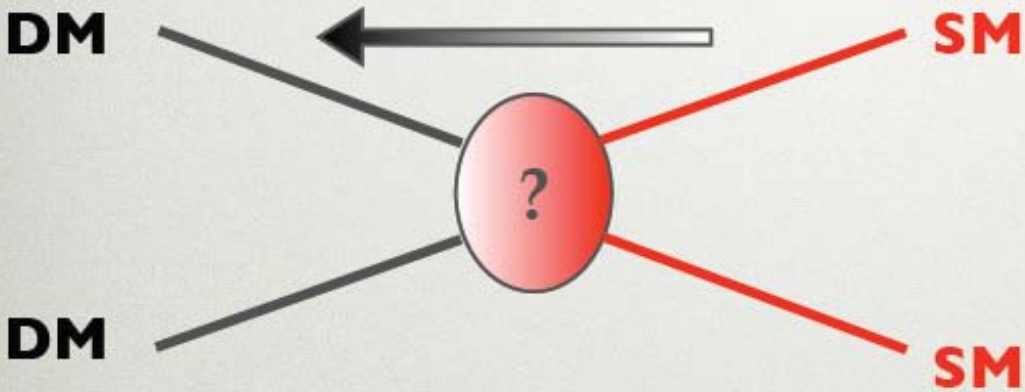

Dark Matter WIMP Searches

COLLIDER SEARCHES

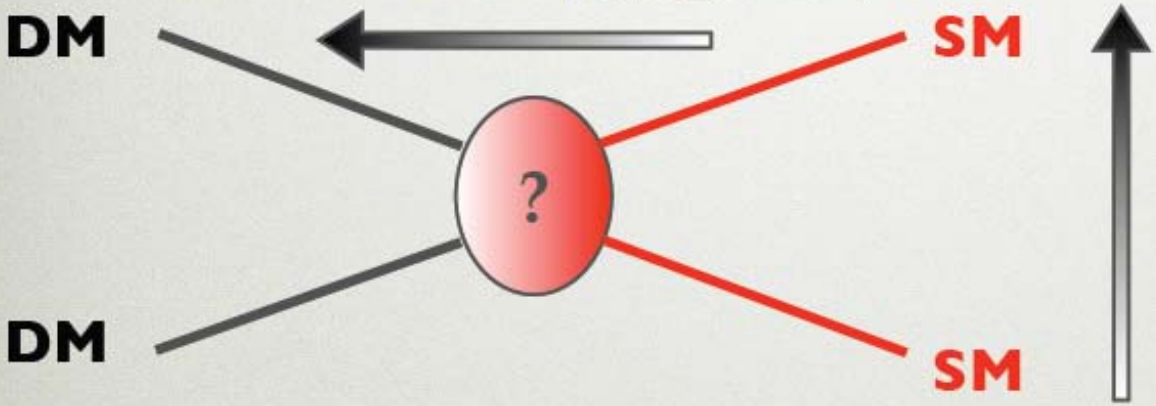

DIRECT SEARCHES

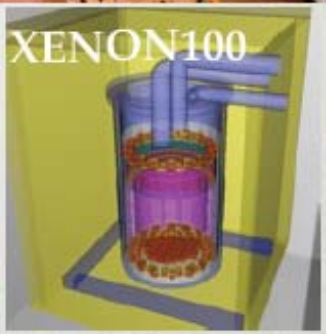

Dark Matter WIMP Searches

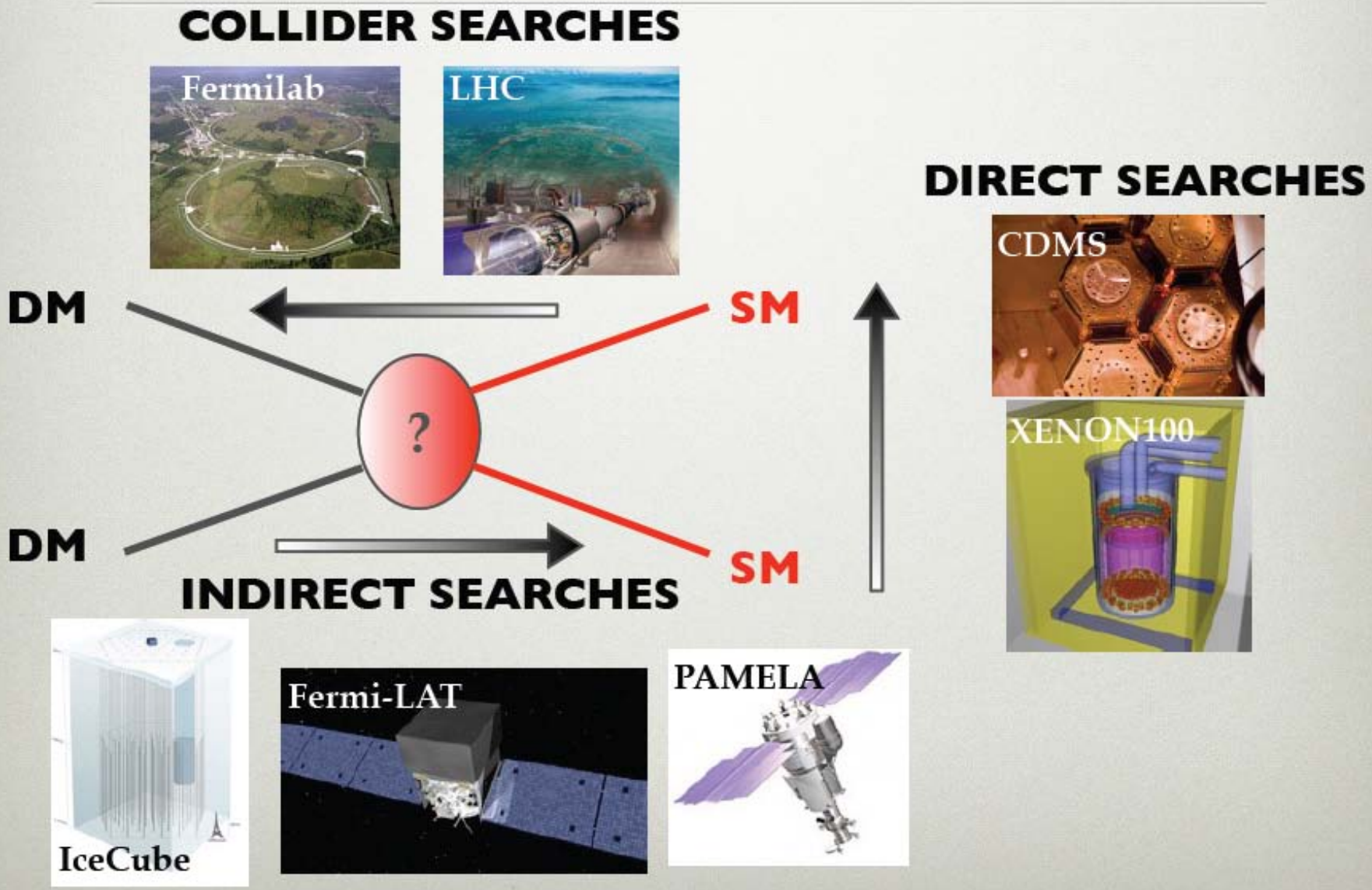

Fermi Gamma Ray Space Telescope

Two Instruments:

LAT: 20 MeV →300 GeV

GBM: 10 keV →30 MeV

Launch: June 11, 2008

5-year mission (10-year goal)

LEO @ 565km, 25.6^{o} orbit inclination

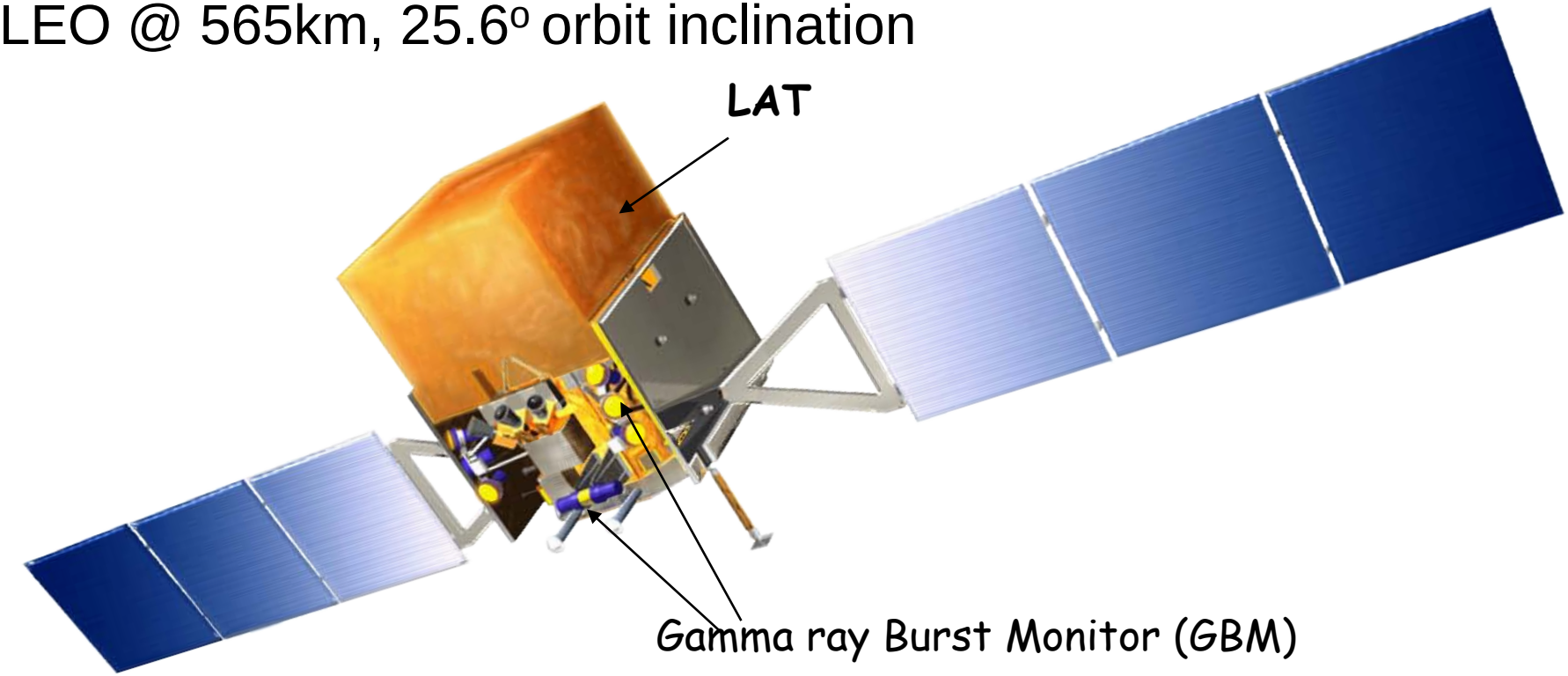

spacecraft partner:
General Dynamics

The LAT

Pair conversion telescope

Precision Si-strip Tracker:
precise measurement of photon direction, photon ID.
Si strip detectors, W conversion foils; 80 m^2 of Si active area. 1.5 radiation lengths on-axis.

Hodoscopic CsI Calorimeter:
measurement of photon energy, shower imaging.
Array of 1536 CsI(Tl) crystals in 8 layers. 8.6 radiation lengths on-axis.

Segmented Anti-Coincidence Detector (ACD):
charged particle veto (0.9997 average detection efficiency). Segmented design reduces self-veto at high energy.
89 plastic scintillator tiles and 8 ribbons.

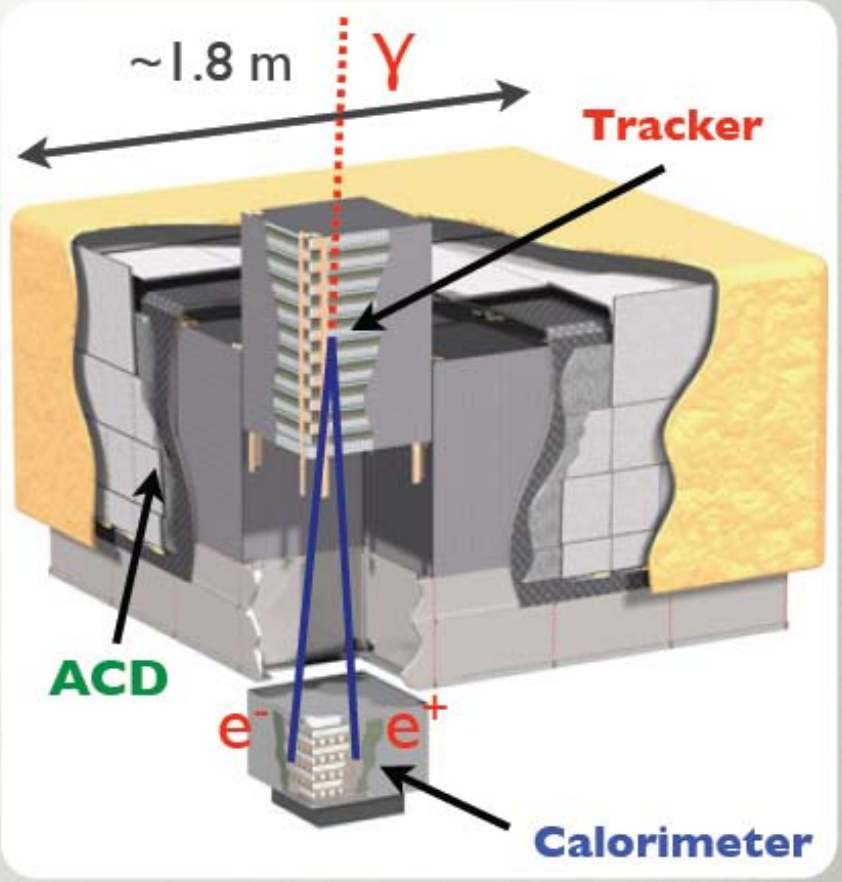

Fermi-LAT as a Telescope

- Shh: *It isn't one*
- However, it is an astounding machine – a massive particle physics detector in orbit
- 1.8 x 1.8 m^2, 3 metric tons, moving at 17,000 miles/hr
- Position knowledge to few m, attitude to ~10″, time to <10 μs
- FoV >120 deg across (20% of the sky)
- "It uses less power than a toaster and we talk to it over a telephone line." (Bill Atwood)
- Cosmic-ray background is intense; onboard filtering is essential (~10^{-6} rejection of background for the cleanest photon classes).

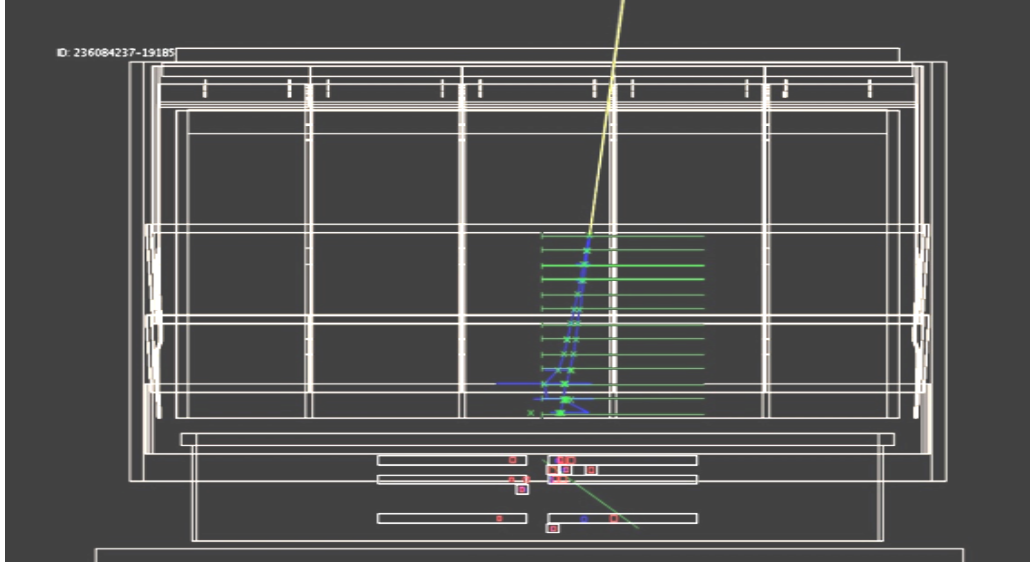

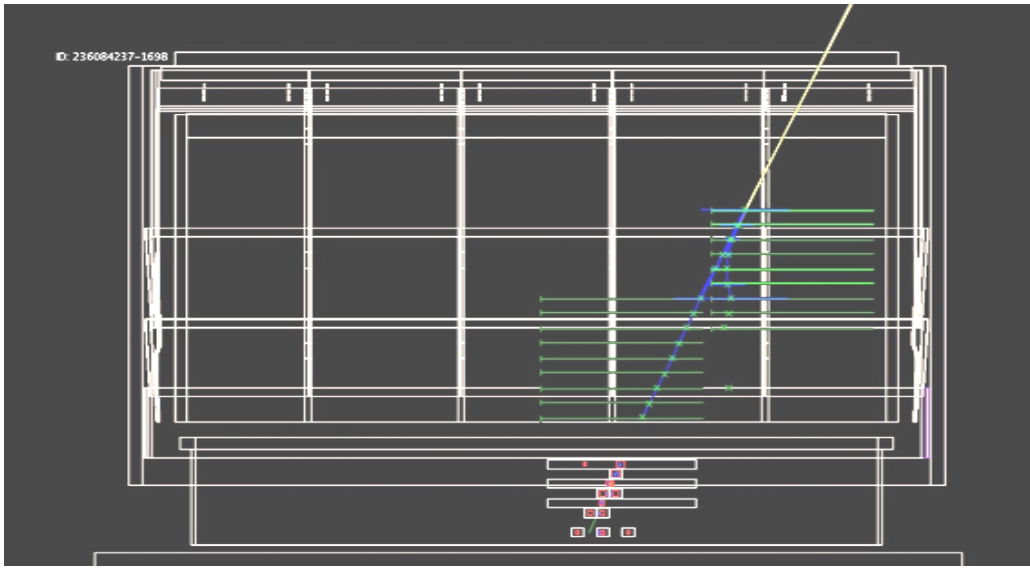

Single Events classified as γ rays

The Observatory

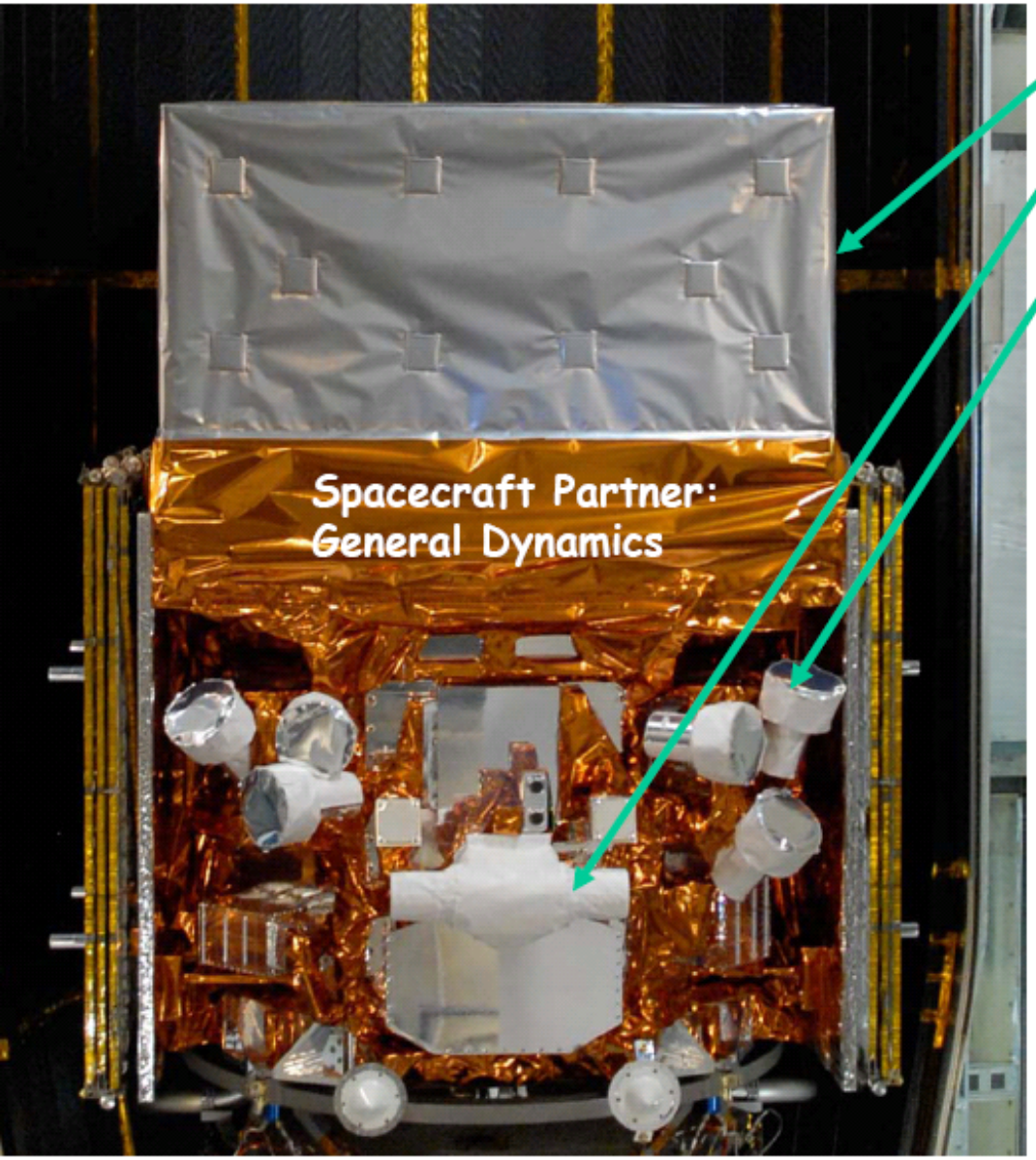

Large AreaTelescope (LAT)
20 MeV - >300 GeV

Gamma-ray Burst Monitor (GBM)
NaI and BGO Detectors
8 keV - 40 MeV

KEY FEATURES

- Huge field of view
  - –LAT: 20% of the sky at any instant; in sky survey mode, expose all parts of sky for ~30 minutes every 3 hours. GBM: whole unocculted sky at any time.
- Huge energy range, including largely unexplored band 10 GeV - 100 GeV.

Total of >7 energy decades!

FGST Prior to Fairing Installation

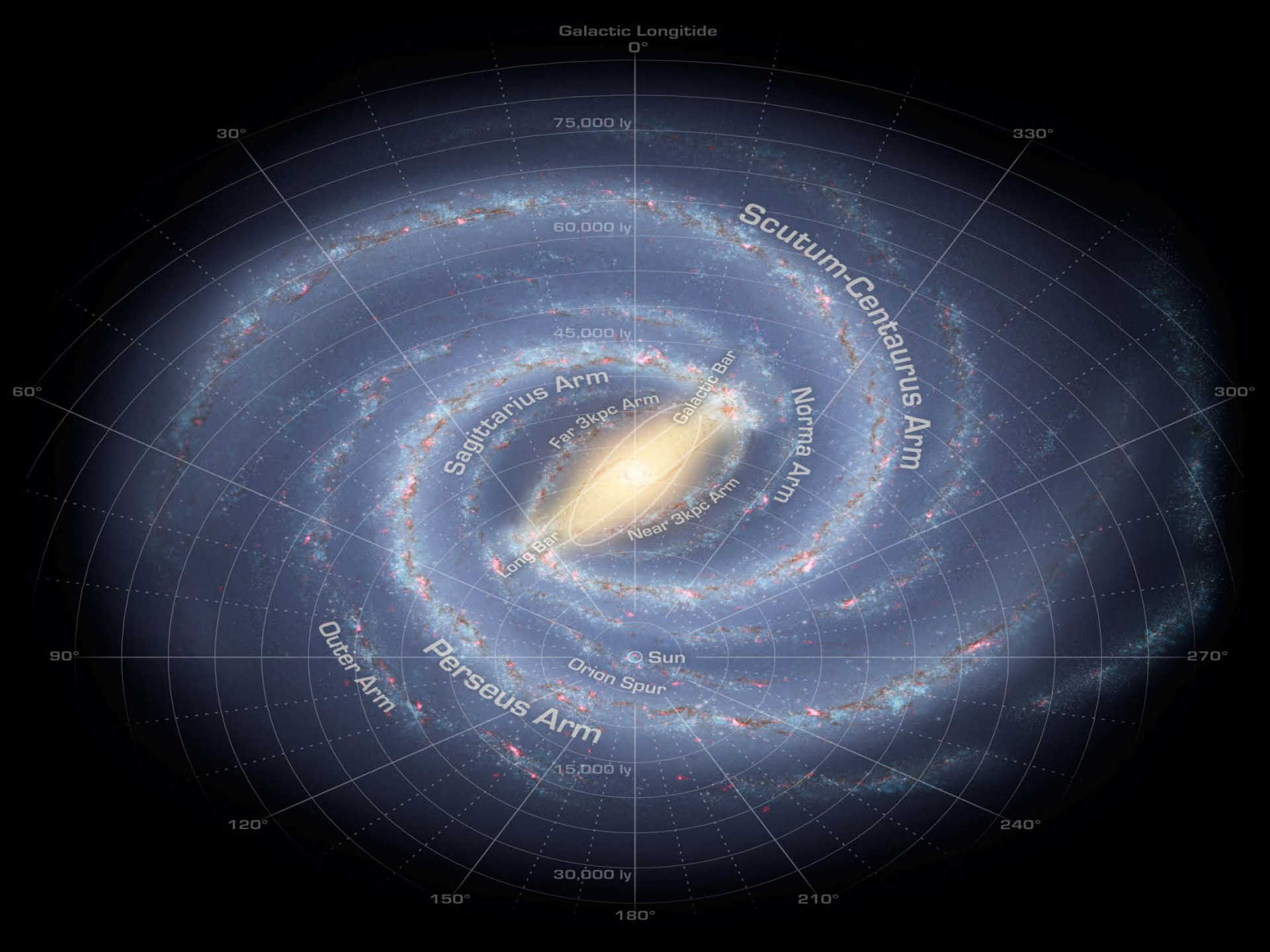
Galactic Longitide
0°
30°
330°
60°
300°
90°
270°
120°
240°
150°
210°
180°
75,000 ly
60,000 ly
45,000 ly
30,000 ly
15,000 ly
Scutum-Centaurus Arm
Sagittarius Arm
Far 3kpc Arm
Galactic Bar
Norma Arm
Near 3kpc Arm
Long Bar
Outer Arm
Perseus Arm
Sun
Orion Spur

Sky Image is for Energies > 1 GeV

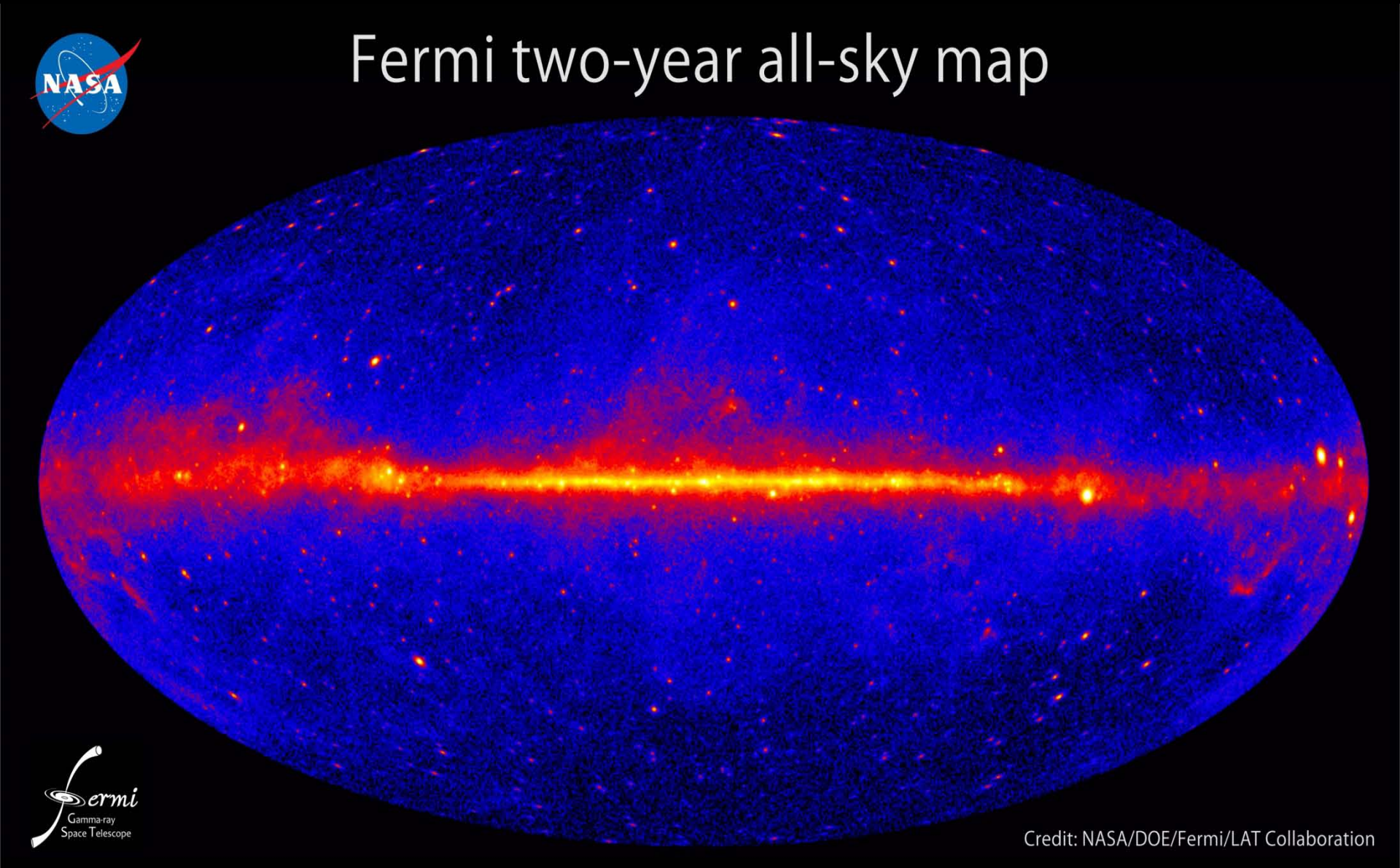

The Fermi LAT 1FGL Source Catalog

1,451 sources (ApJ Supplement Series, 188:405–436, 2010 June)

Description	Designator	Number Assoc. (ID)
Pulsar, X-ray or radio, identified by pulsations	psr (PSR)	7 (56)
Pulsar, radio quiet (LAT PSR, *subset of above*)	PSR	24
Pulsar wind nebula	pwn (PWN)	2 (3)
Supernova remnant	† (SNR)	41 (3)
Globular Cluster	glc (GLC)	8 (0)
Micro-quasar object: X-ray binary (black hole or neutron star) with radio jet	mqo (MQO)	0 (1)
Other X-ray binary	hxb (HXB)	0 (2)
BL Lac type of blazar	bzb (BZB)	295 (0)
FSRQ type of blazar	bzq (BZQ)	274 (4)
Non-blazar active galaxy	agn (AGN)	28 (0)
Active galaxy of uncertain type	agu (AGU)	92 (0)
Normal galaxy	gal (GAL)	6 (0)
Starburst galaxy	sbg (SBG)	2 (0)
Unassociated		630

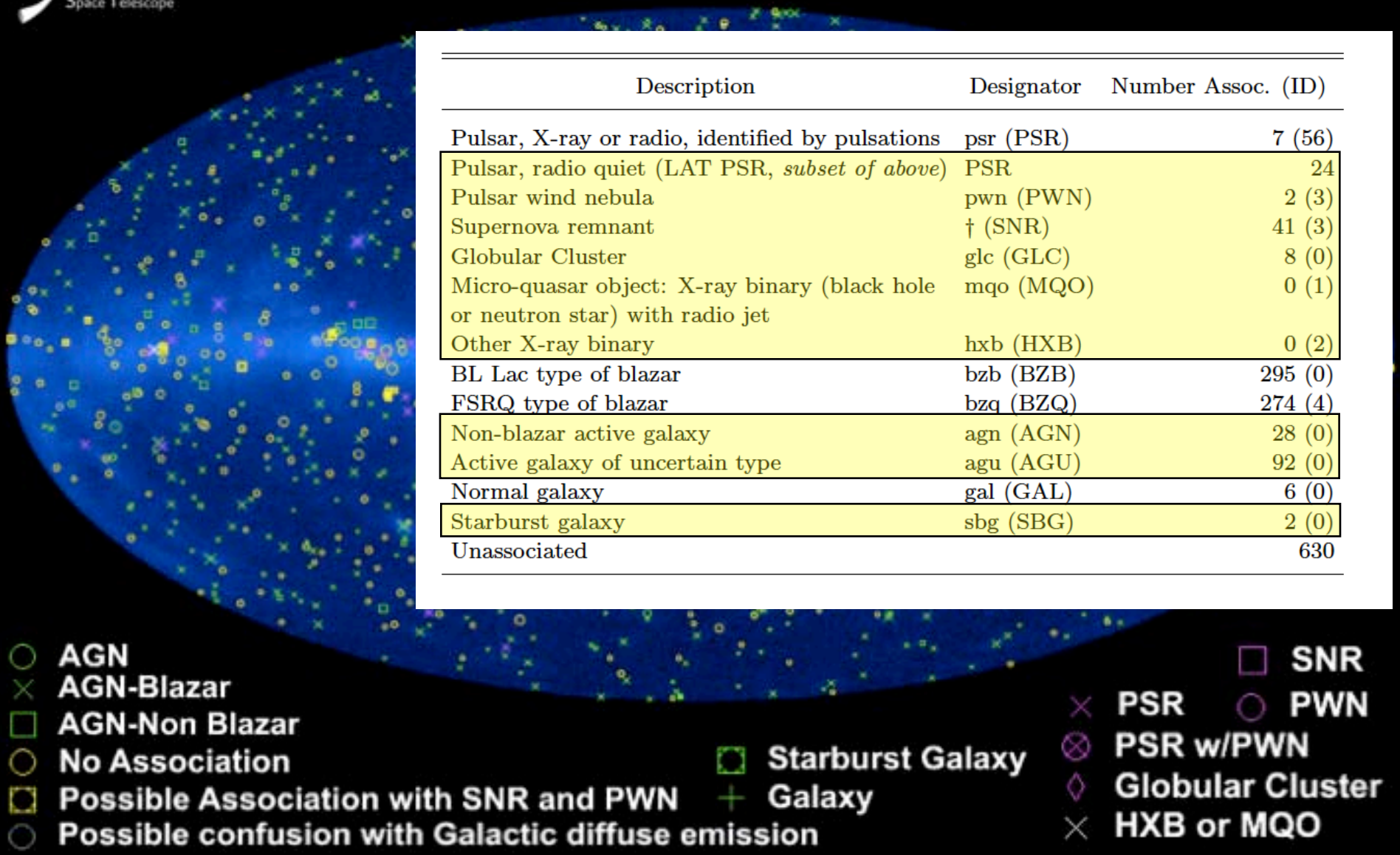

Credit: *Fermi* Large Area Telescope Collaboration

Gamma-Ray Lobes

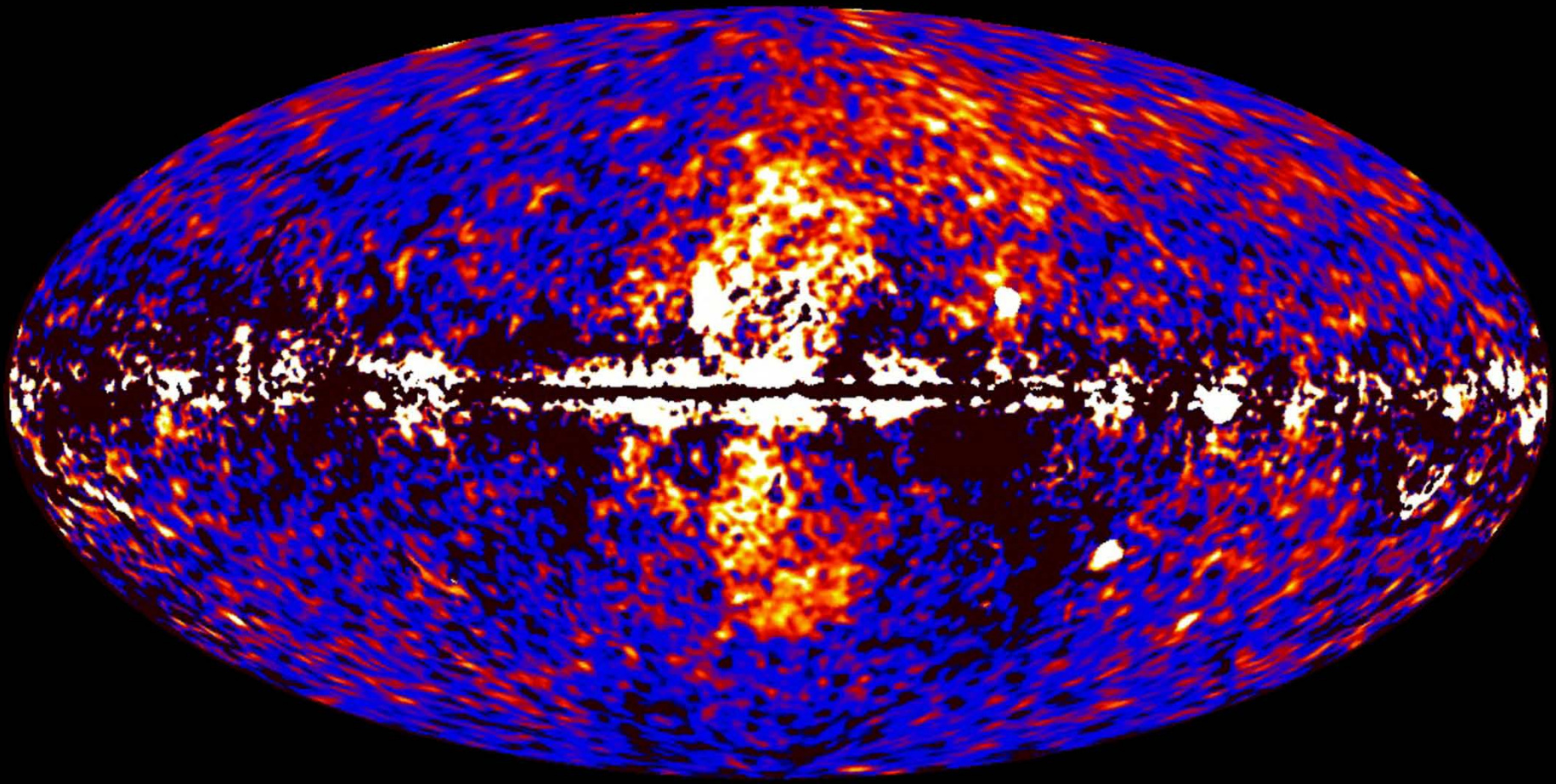

The new structure consists of enormous bubbles extending about 50° north and south of the Galactic center.

Su, Slatyer and Finkbeiner, 2010

Via Lactea – II
The Milky Way Dark Matter Halo
(viewed from far far away)

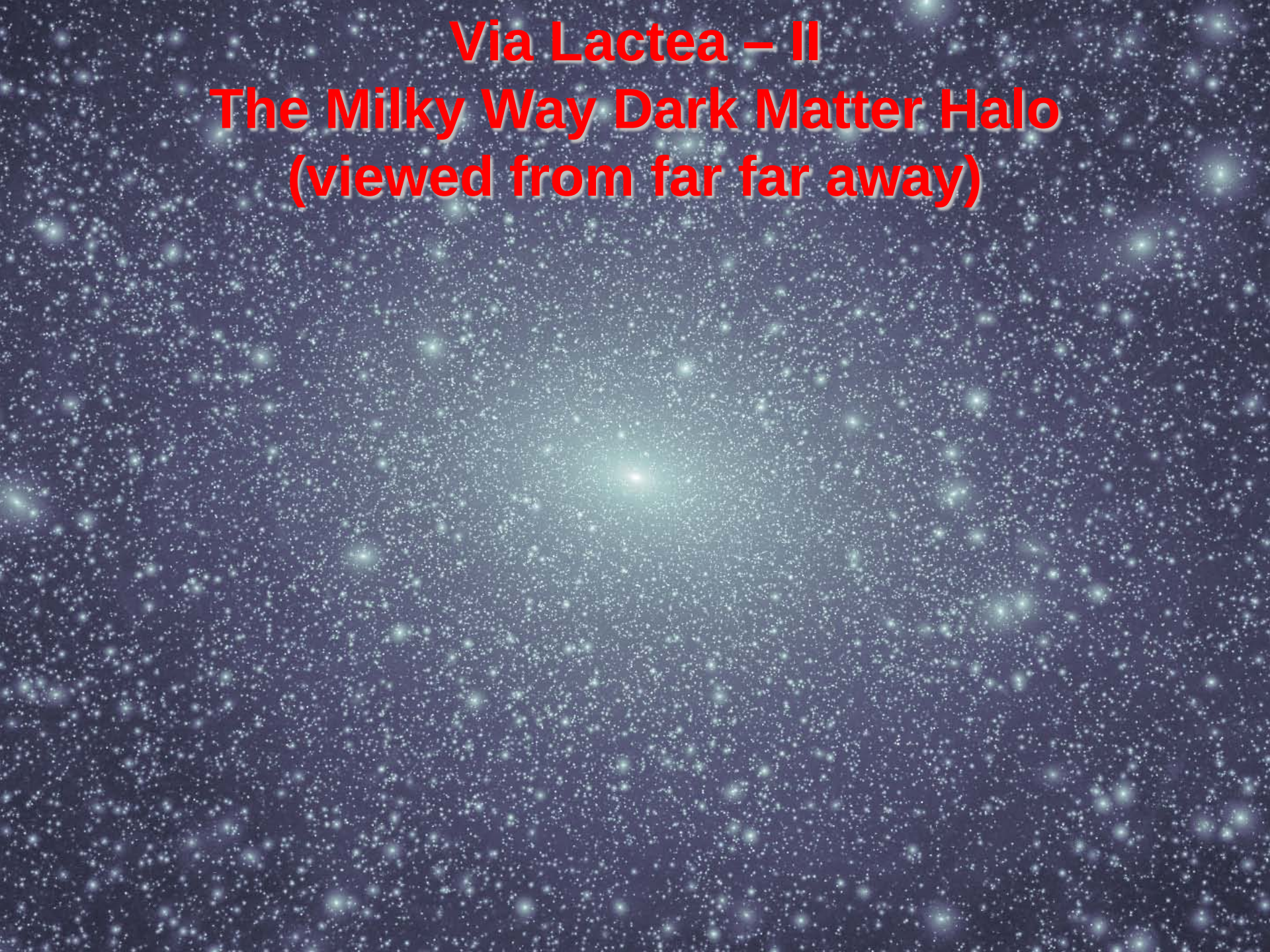

Dark Matter Distribution

- The dark matter annihilation (or decay) signal strongly depends on the dark matter distribution.
- Cuspier profiles and clumpiness of the dark matter halo can provide large boost factors

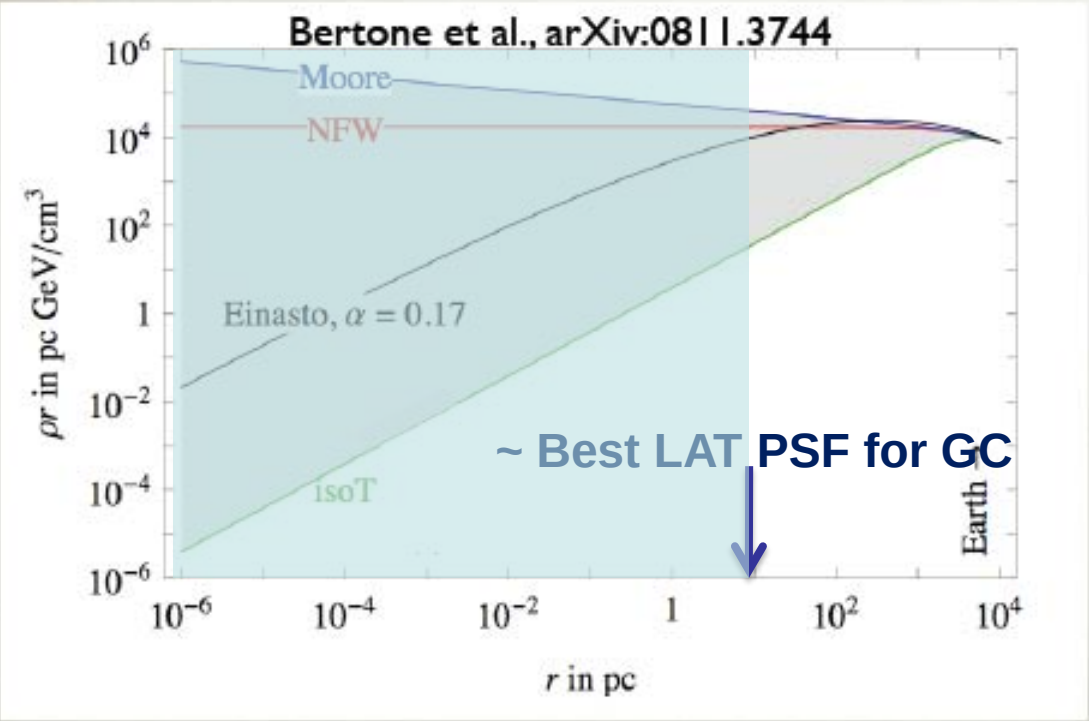

NFW profile

$$\rho(r) = \rho_0 \frac{r_0}{r} \frac{1 + (r_0/a_0)^2}{1 + (r/a_0)^2}$$

$$\rho_0 = 0.3 \text{ GeV/cm}^3$$
$$a_0 = 20 \text{ kpc}, \; r_0 = 8.5 \text{ kpc}$$

- ✓ Via Lactea II predicts a cuspier profile, $\rho(r) \propto r^{-1.2}$
- ✓ Aquarius predicts a shallower than r^{-1} innermost profile

Fermi Search Strategies

Galactic center:
Good statistics but source confusion/diffuse background

Satellites:
Low background and good source ID, but low statistics

Milky Way halo:
Large statistics but diffuse background

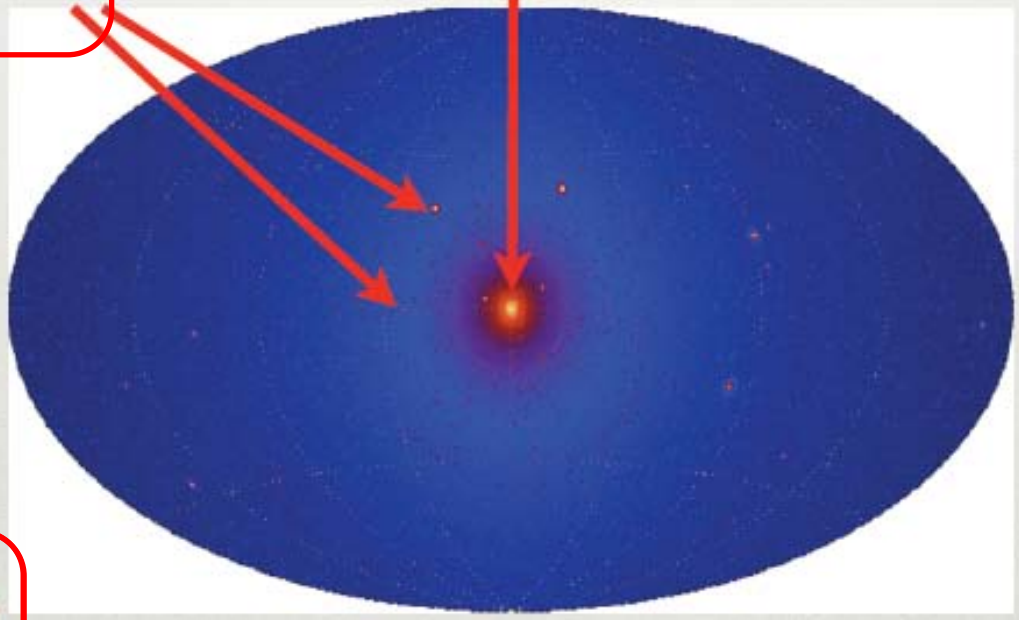

All-sky map of gamma rays from DM annihilation arXiv:0908.0195 (based on Via Lactea II simulation)

And electrons!

Spectral lines:
No astrophysical uncertainties, good source ID, but low statistics

Galaxy clusters:
Low background but low statistics

Extragalactic:
Large statistics, but astrophysics, Galactic diffuse background

Pre-launch sensitivities published in Baltz et al., 2008, JCAP 0807:013 [astro-ph/0806.2911]

Fermi-LAT publications

- High-level papers (121 refereed publications since launch, i.e. 3.7 per month)

Category I and II papers in refereed journals

Journal	Published	In press	Total
Astronomy and Astrophysics	4+2=6	-	6
Astroparticle Physics	1+2=3	-	3
Astrophysical Journal	52+7=59	1+1=2	61
Astrophysical Journal Letters	17+4=21	-	21
Astrophysical Journal Supplement	3+0=3	0+1=1	4
Journal of Cosmology and Astroparticle Physics	2+2=4	-	4
Monthly Notices of the RAS	-	0+3=3	3
Nature	2+0=2	-	2
Physical Review D	3+0=3	-	3
Physical Review Letters	4+0=4	-	4
Science	10+0=10	-	10
Total	98+17=115	1+5=6	121

The highest-cited paper: Cosmic Ray Electrons

Fermi-LAT

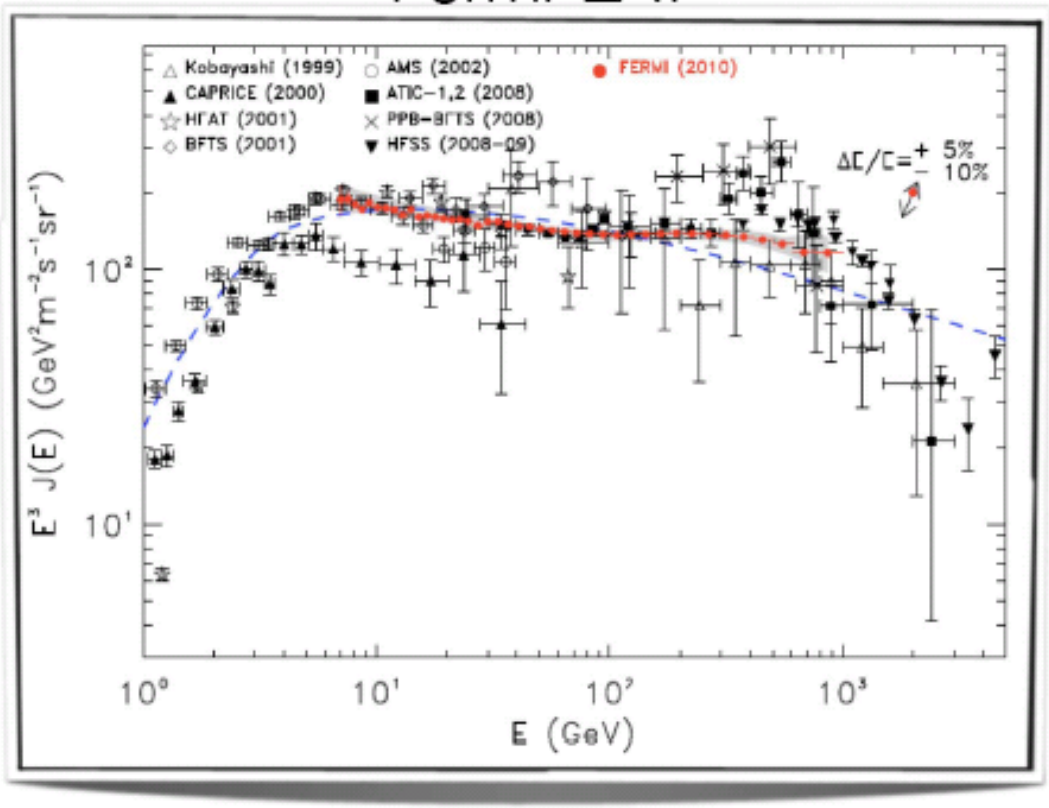

H.E.S.S.

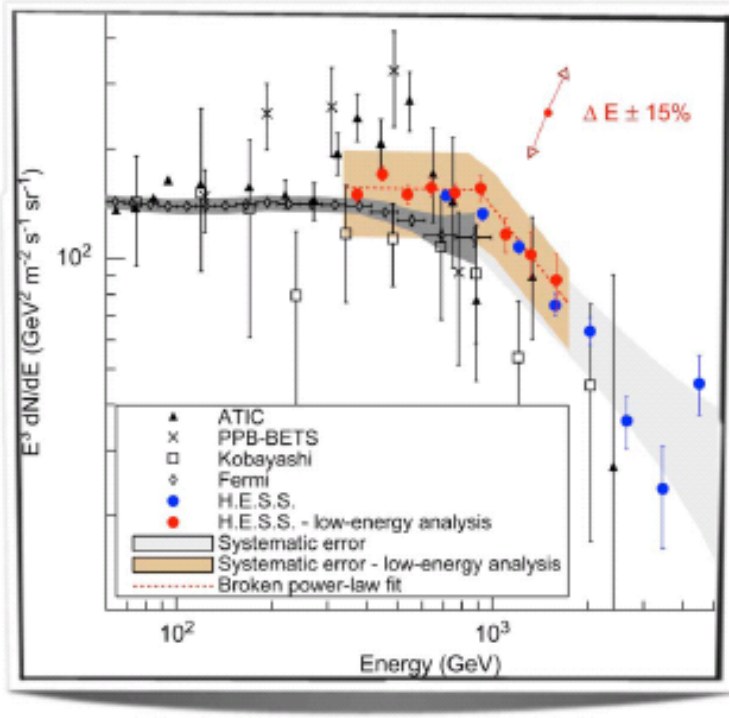

- Possibility to detect DM signatures not only in the gamma-rays but also in charged particles

Measurement of the cosmic ray e+ + e- spectrum from 20 GeV to 1 TeV with the Fermi Large Area Telescope Abdo, A. A. et al. 2009, Phys. Rev. Lett., 102, 181101. 444 citations

On possible interpretations of the high energy electron-positron spectrum measured by the Fermi Large Area Telescope Grasso, D. et al. 2009, Astropart. Phys., 32, 140. 111 citations

Fermi's

... Next step: Electron/Positron separation

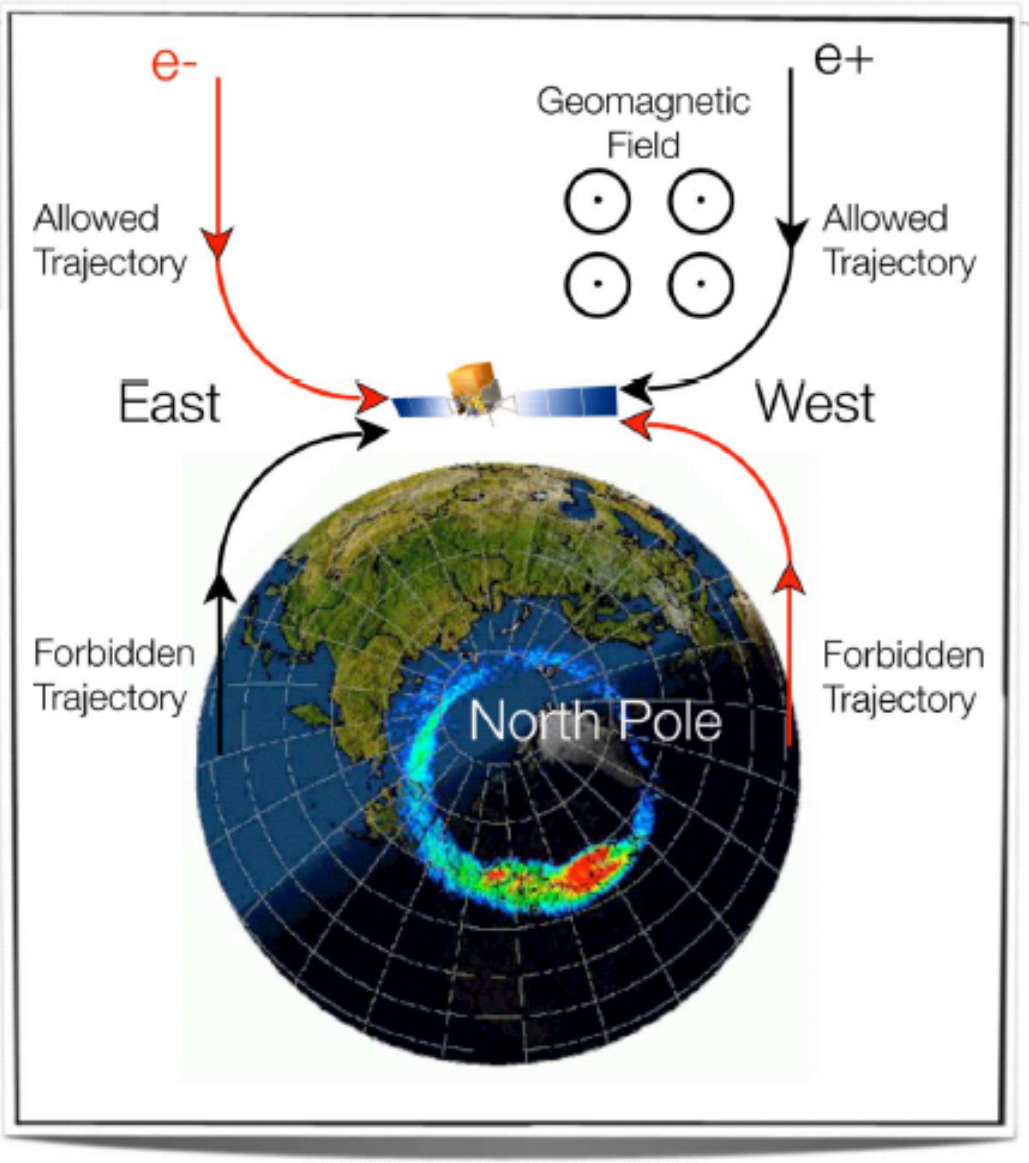

PAMELA, Nature 458, 607 (2009)

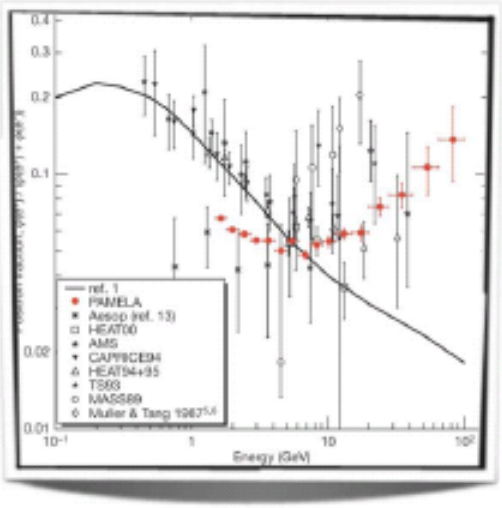

Photons from WIMP Annihilation

$$\frac{d\Phi_\gamma}{dE_\gamma}\left(E_\gamma,\phi,\theta\right)=\frac{1}{4\pi}\frac{\langle\sigma_{ann}v\rangle}{2m_\chi^2}\sum_f\frac{dN_\gamma^f}{dE_\gamma}B_f \times\int_{\Delta\Omega(\phi,\theta)}d\Omega'\int_{los}\rho^2\left(\vec{r}\left(l,\theta',\phi'\right)\right)dl$$

Particle Physics

J ≡ DM Distribution

- Charged particles are more complicated (need to include propagation, energy losses)

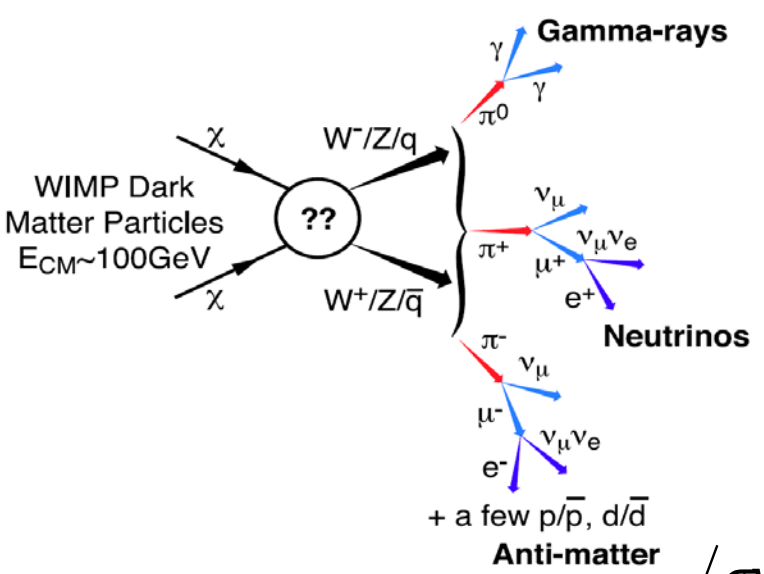

Spectral line

Prompt annihilation into γγ, γZ, γH⁰...
(also prompt decay into photons)

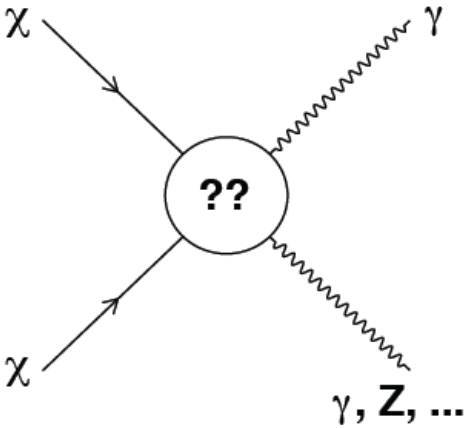

Note: For a decaying DM particle $\frac{\langle\sigma v\rangle}{2m^2}\rho^2 \rightarrow \frac{1}{m\tau}\rho$

Extragalactic diffuse emission

- Contains contribution from sub-threshold sources
- Global fit (Galactic diffuse, sources, isotropic)
- Softer than previously thought (smaller contribution to electron spectrum at TeV energies). Difference to EGRET can be explained by more resolved source

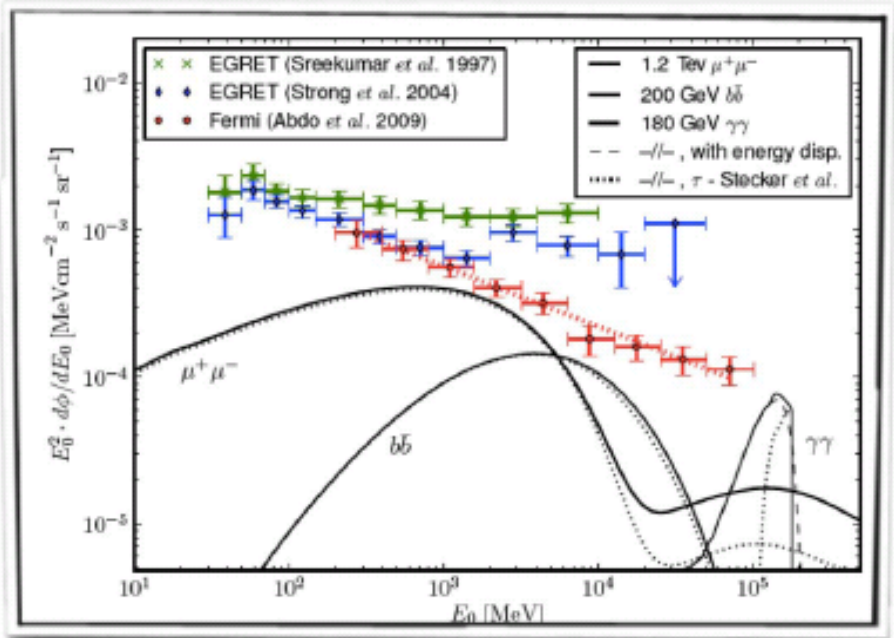

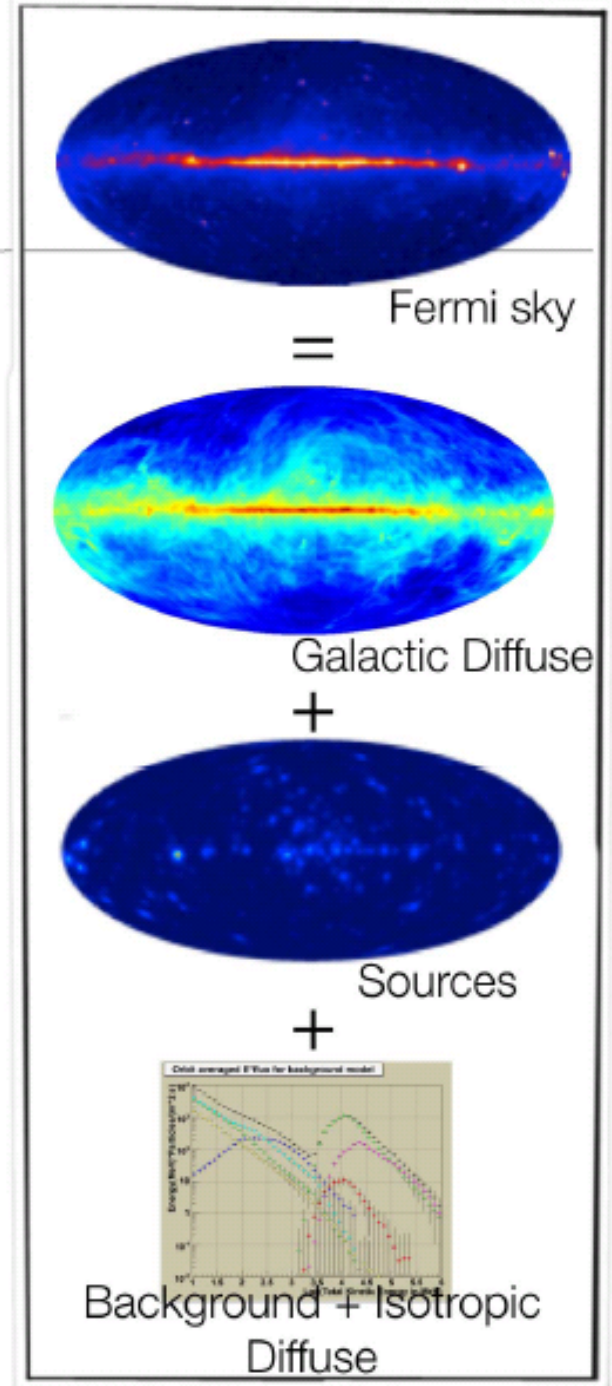

The extragalactic background diffuse emission (EGB)

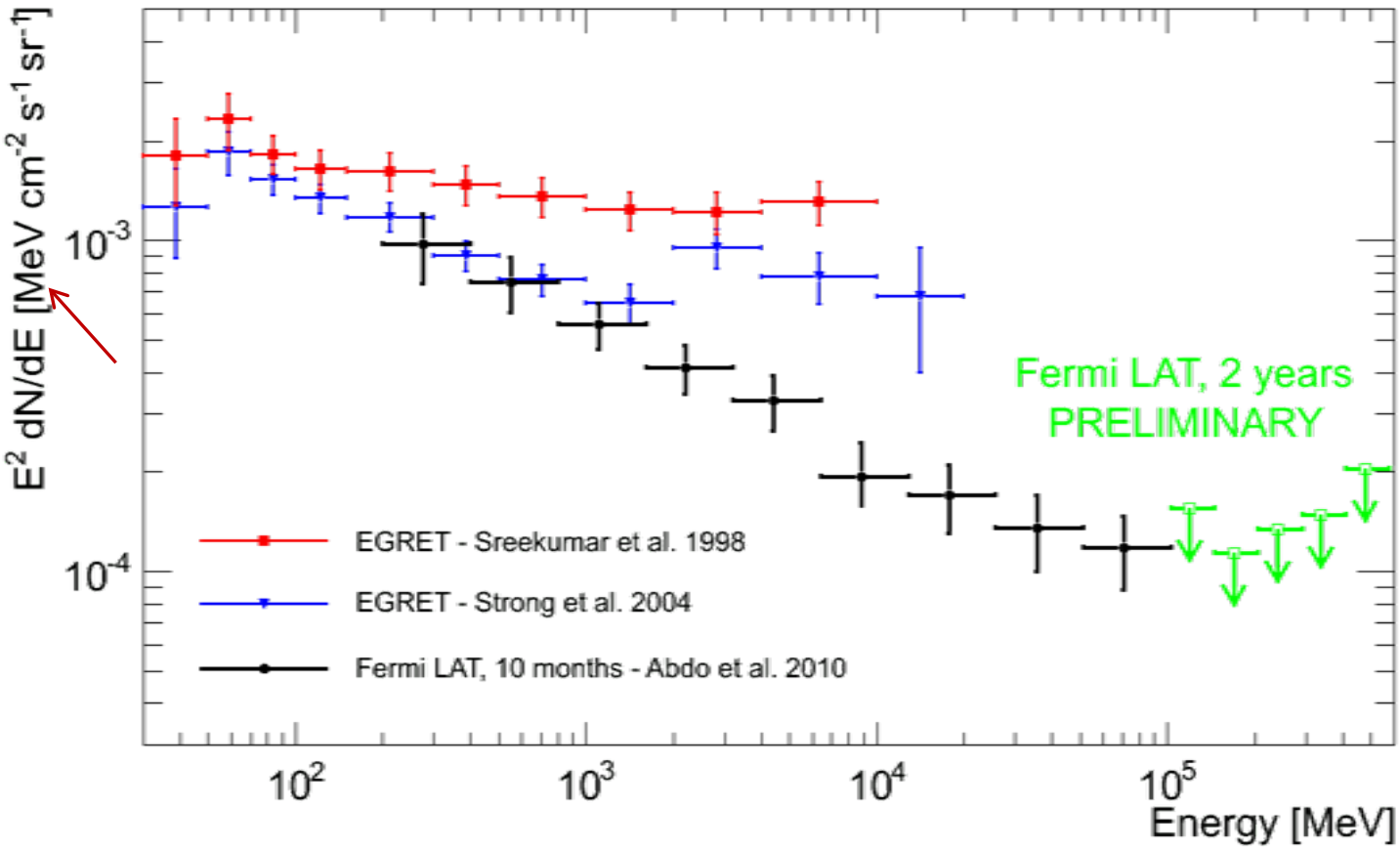

For E> 100 GeV the limits are 95% upper limits and include a 20% uncertainty on the LAT effective area at high energies

- >100 GeV the Fermi LAT Monte Carlo simulation of residual CR contamination was too statistically limited to allow an accurate subtraction of this background. Only upper limits on the EGB are shown.
- A more robust energy estimator is used above 100 GeV instead of the standard LAT reconstructed energy.
- E> 100 GeV we only use regions of the sky for which the EGB is the dominant component of the diffuse emission.
- Regions within 1.5 deg of LAT 1FGL catalog sources were cut.

Extragalactic diffuse emission

- Case A: be completely agnostic about the Fermi-LAT sky and assume that all of the extragalactic diffuse emission is generated by DM annihilation (i.e. only require that the DM annihilation channel is below the measurement)

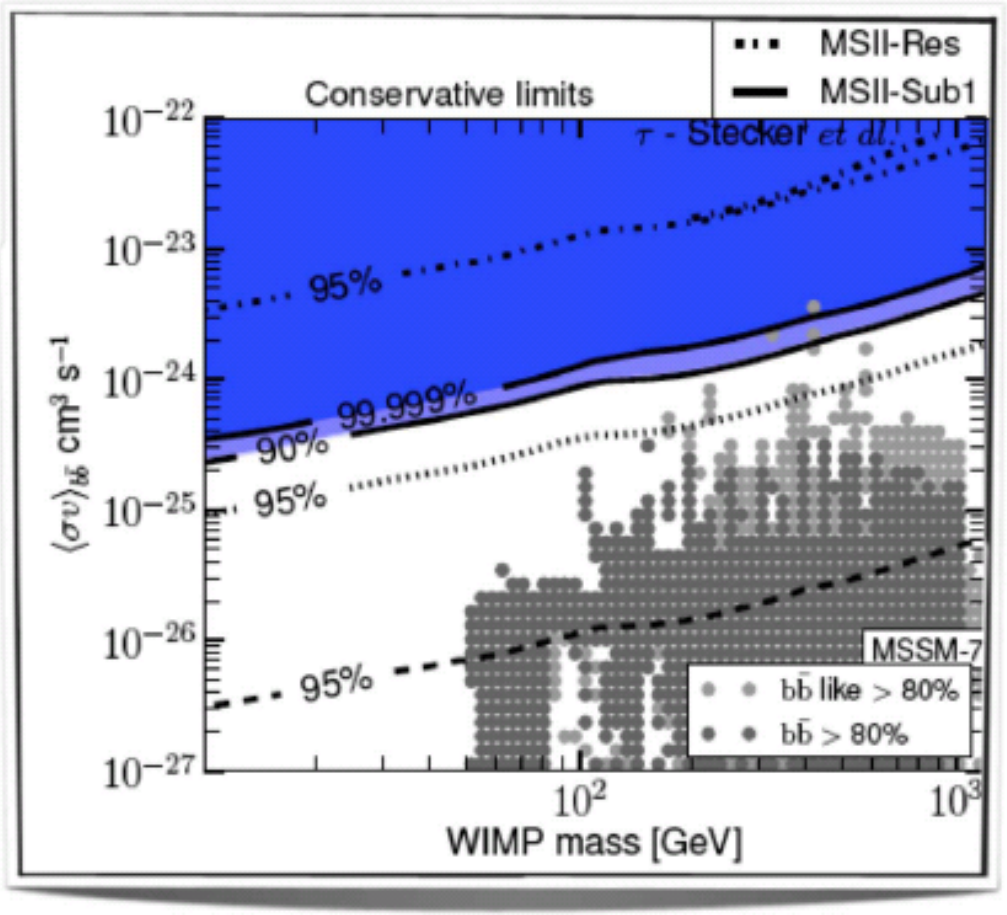

Abdo, A. A. et al. 2010, JCAP, 04, 014

Extragalactic diffuse emission

- Case B: Can do better by subtracting the known population contribution using logN - logS to extrapolate below Fermi source detection flux values.
  - explains ~ 30% of extra galactic diffuse
  - additional contributions from star forming galaxies, GRBs, … dark matter.

Abdo, A. A., et al. 2010, ApJ. **720**, 435

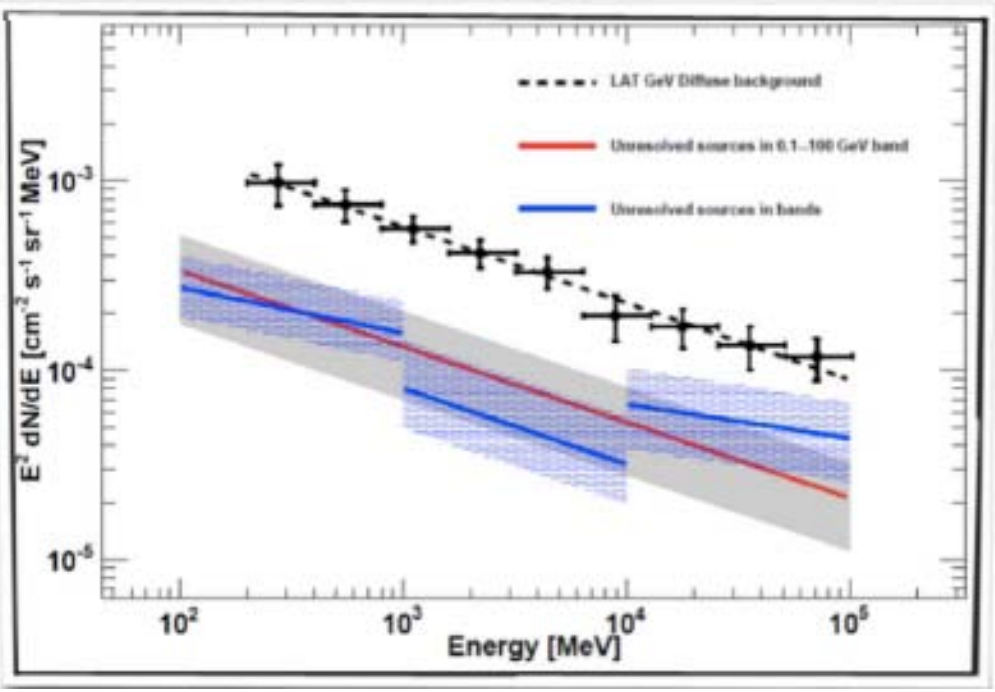

Composition of the |b| ≥20 TS≥50 sample used in this analysis.

CLASS	# objects
Total	425
FSRQs	161
BL Lacs	163
Uncertain[a]	4
Blazar Candidates	24
Radio Galaxies	2
Pulsars	9
Others[b]	6
Unassociated sources	56

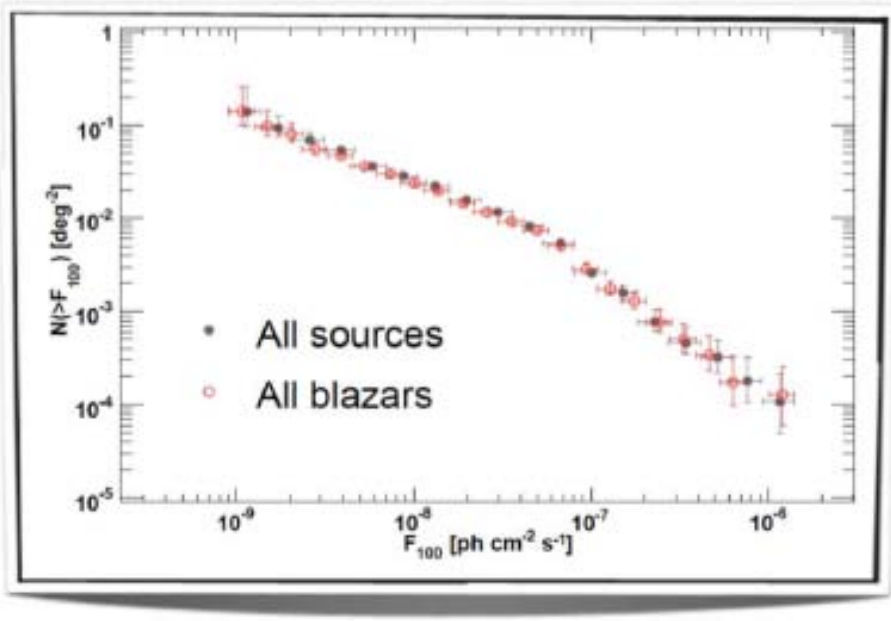

All sources = 425 = Total
All blazars = [Σ(#red)]*(1+#UnS/Total)
Curves overlap ⇒ UnS are mostly blazars.

Extragalactic diffuse emission

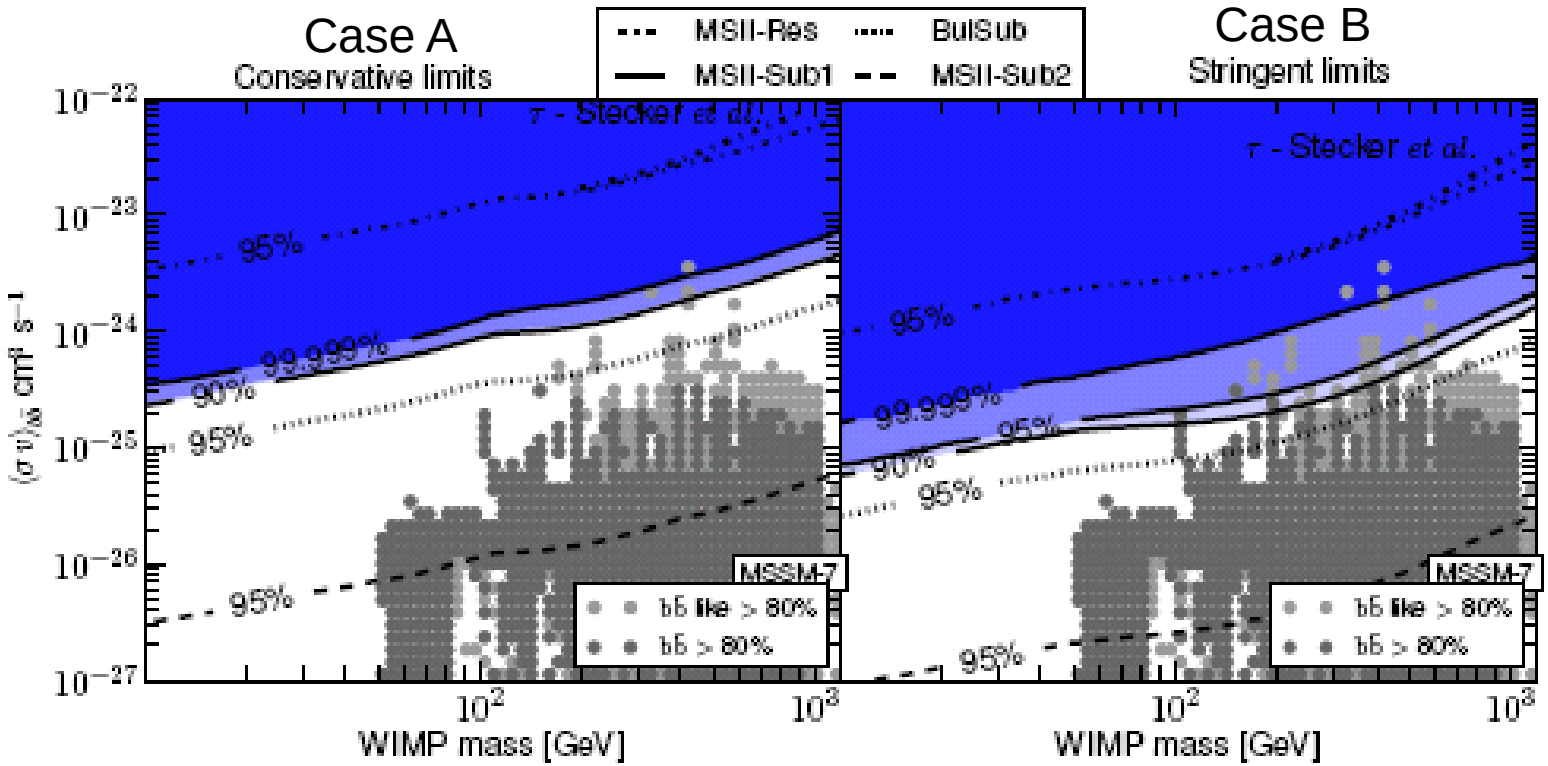

Figure 5. Cross section $\langle \sigma v \rangle$ limits on dark matter annihilation into $b\bar{b}$ final states. The blue regions mark the (90, 95, 99.999)% exclusion regions in the MSII-Sub1 $\Delta^2(z)$ DM structure scenario (and for the other structure scenarios only 95% upper limit lines). The absorption model in Gilmore et al. [68] is used, and the relative effect if instead using the Stecker et al. [69] model is illustrated by the upper branching of the dash-dotted line in the MSII-Res case. Our *conservative* limits are shown on the left and the *stringent* limits on the right panel. The grey regions show a portions of the MSSM7 parameter space where the annihilation branching ratio into final states of $b\bar{b}$ (or $b\bar{b}$ like states) is $> 80\%$. See main text for more details.

Abdo, A. A. et al. 2010, JCAP, 04, 014

Comparison of the Extragalactic Diffuse γ –ray Background[1] to Calculations of Contributions from Blazars[2] + Star-forming Galaxies[3]

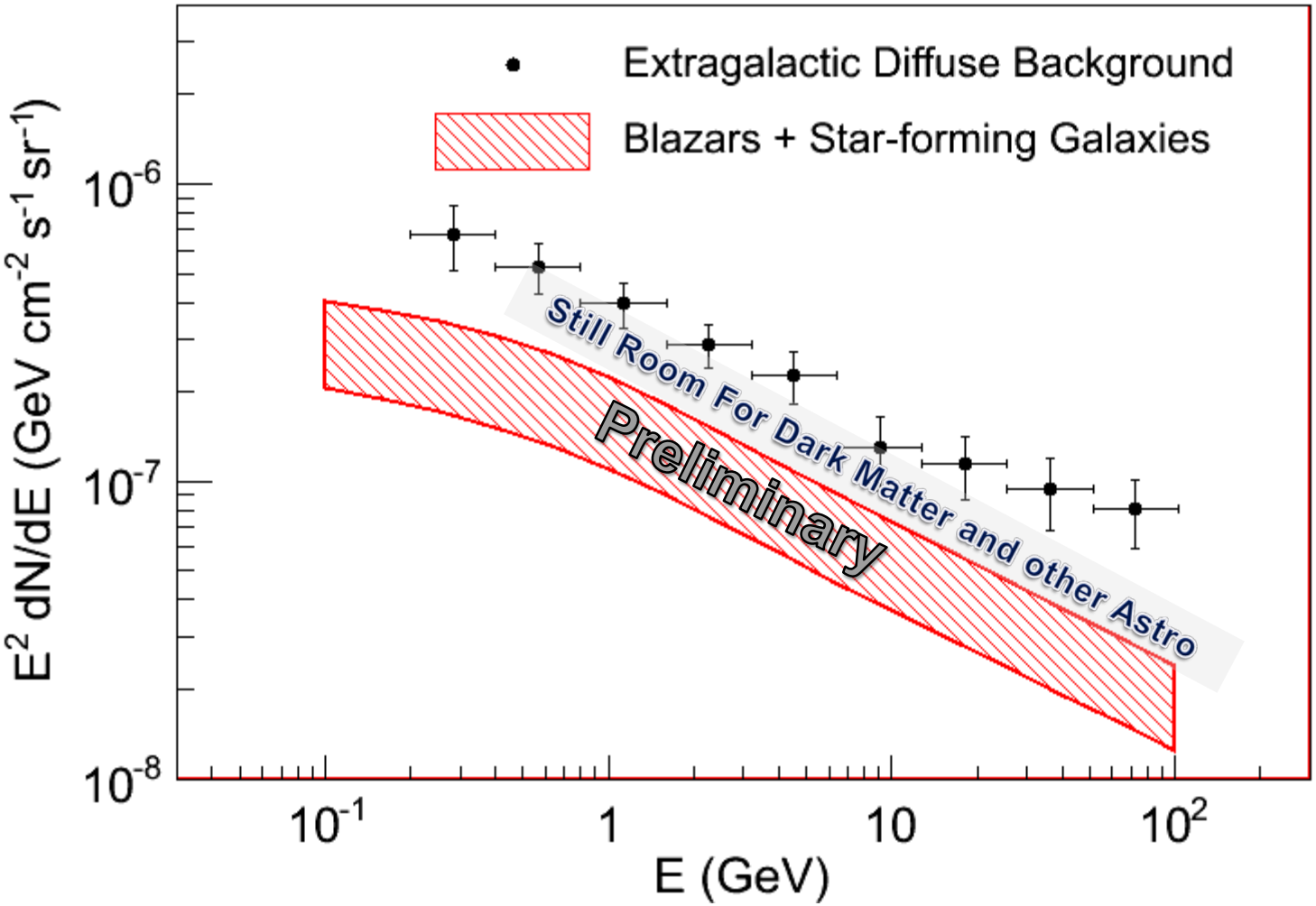

1) Abdo, A. A. et al. 2010, Phys. Rev. Letts. **104**, 101101;

2) Abdo, A. A., et al. 2010, ApJ. **720**, 435; 3) Fermi LAT Collaboration Preliminary.

DM Subhalos

- DM substructures: very low background targets for DM searches a “smoking gun” signal.

- Optically observed dwarf spheroidal galaxies (dSph): largest clumps predicted by N-body simulation.
  - Very large M/L ratio: 10 to ~> 1000 (M/L ~ 6-10 for Milky Way)
  - More promising targets could be discovered by current and upcoming experiments! (SDSS, DES, PanSTARRS, ...)
  - Great targets for gamma ray observations as most are expected to be free from other astrophysical gamma ray sources and have low content in dust/gas, very few stars

- ultra-faint dwarfs
- classical dwarfs

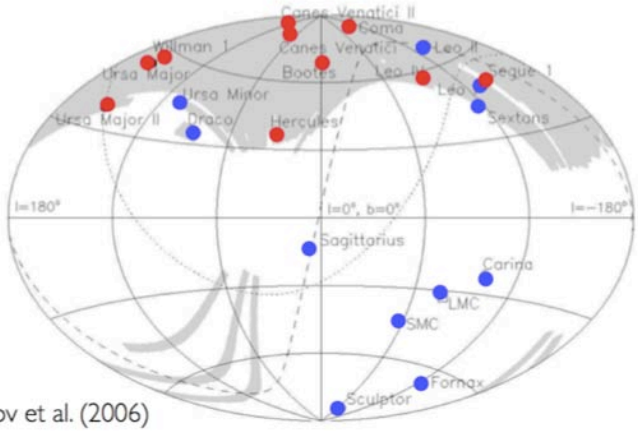

Belokurov et al. (2006)

- Never before observed DM substructures (DM satellites):
  - Would significantly shine only in radiation produced by DM annihilation/decay
  - Some of these satellites could be within a few kpc from the Sun (N-body simulations)
  - All sky search for promising candidates with Fermi LAT

Astrophys. J. 712, 147 (2010)

Fermi: Dwarf Spheroidals

- Select promising dSph: less than 180 kpc from the Sun, more than 30° from the Galactic plane, stellar kinematic data.

Ursa Major II
Segue 2
Willman 1
Coma Berenices
Bootes II
Bootes I
Ursa Minor
Sculptor
Draco
Sextans
Ursa Major I
Hercules
Fornax
Leo IV

Astrophys. J. 712, 147 (2010)

Fermi: Dwarf Spheroidals

- No detection by Fermi with 11 months of data.

- Determine 95% flux upper limits for several possible annihilation final states
- Combine with the DM density inferred from the stellar data to extract constraints on the annihilation cross section for a subset of 8 dSph (based on stellar kinematic data)

(Stellar data from the Keck observatory by Martinez, Bullock, Kaplinghat)

Annihilation into bottom quarks

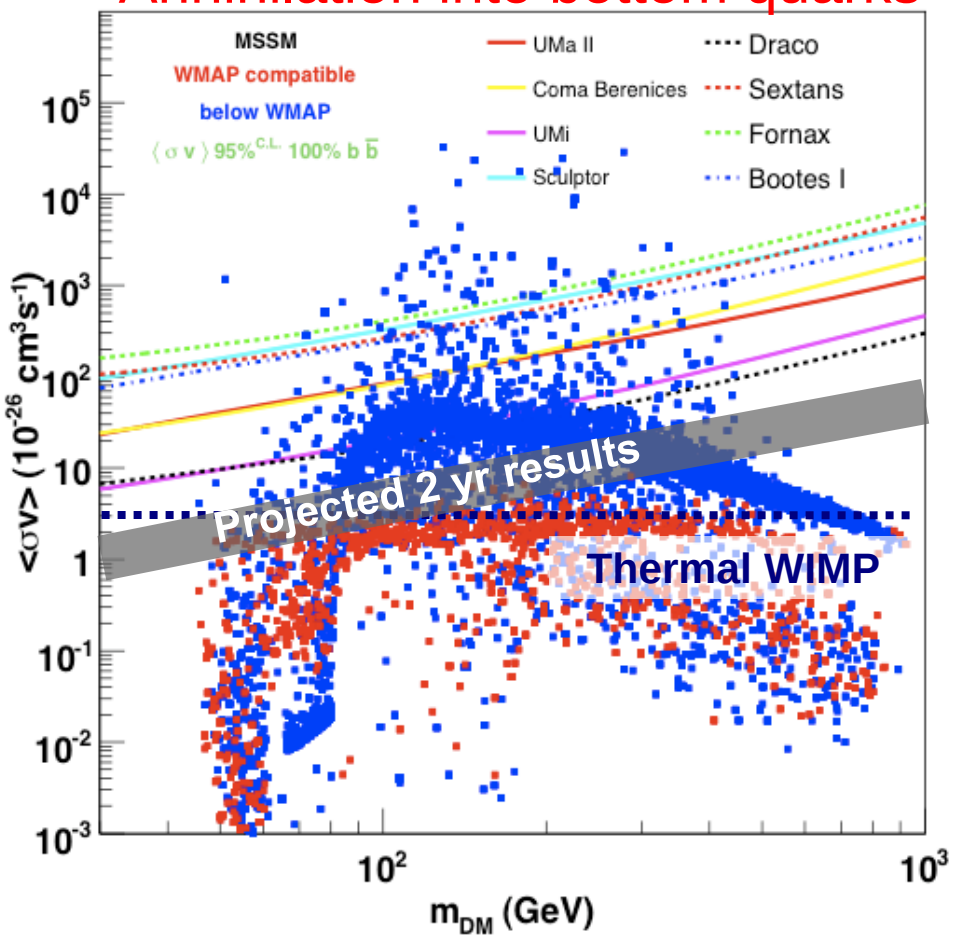

Search For Spectral Lines

- Another Clean signal of dark matter with no astrophysical uncertainties!
- WIMP Annihilations (Decay) $\rightarrow$ $\gamma\nu$, $\gamma\gamma$, γZ, $\gamma H0$, …
- The photon line signal is suppressed in SUSY as internal loops are needed in that case. However, the signal is enhanced in other models such as Inert Higgs, and some gravitino decays.

Particle	Branching Ratios
Neutralino	10^{-3} to 10^{-5}
Inert Higgs Gustafsson, Lundstrom, Bergstrom, Edsjo. March 2007	0.36 to 10^{-4}
Gravitino decay Ibarra, Tran. Sept 2007	0.66 (85 GeV) 0.05 (150 GeV)

Theories with Enhanced Lines (BE)

M. Gustafsson *et al.* [astro-ph/0703512v1]

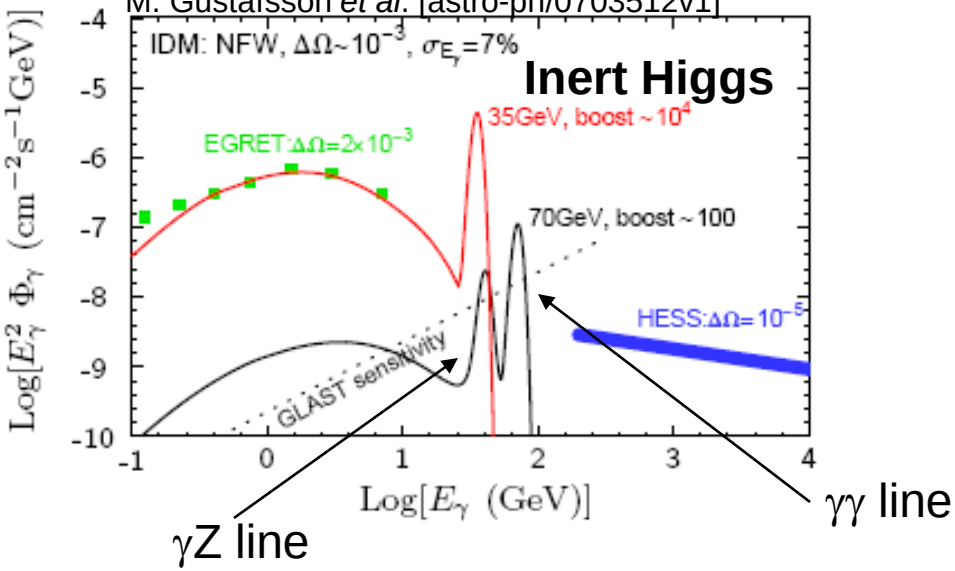

A. Ibarra & D. Tran [astro-ph/0709.4593v1]

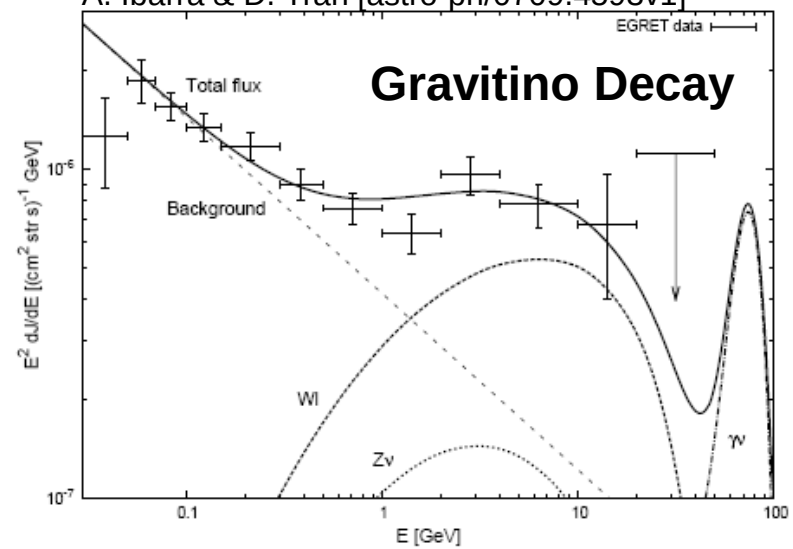

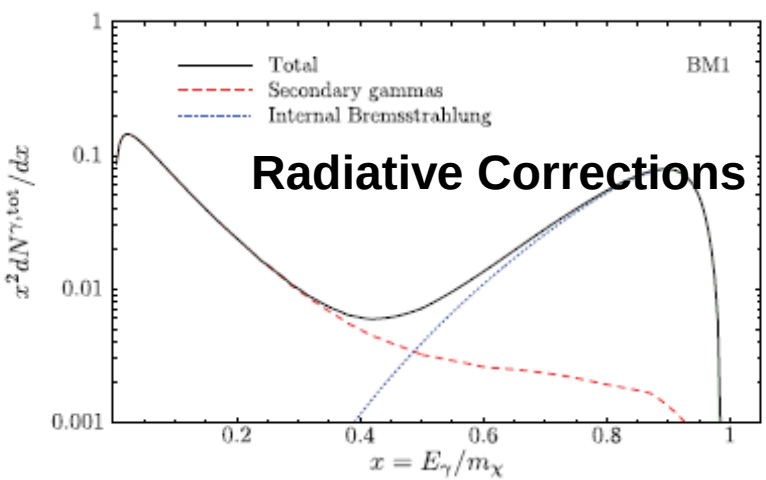

T. Bringmann *et al.* [hep-ph/0710.3169v2]

Particle	Branching Ratios
Neutralino	10^{-3} to 10^{-5}
Inert Higgs Gustafsson, Lundstrom, Bergstrom, Edsjo. March 2007	0.36 to 10^{-4}
Gravitino decay Ibarra, Tran. Sept 2007	0.66 (85 GeV) 0.05 (150 GeV)

Photon Line Search Region of the Sky and Data Selection

- August 7, 2008 - June 30, 2010 – ~23 months of data
- Remove Galactic Plane except for GC: includes (|B|>10) | (|L|<10)
- LAT Profile Energy (fit shower profile assuming cylindrical symmetry) in range [4.8, 264] GeV (the profile energy is not public at this time).
  - Best results for line analysis, not so important for standard astrophysics analyses. Pass 7 coming this year solves the energy measurement issue.
- P6V3 Data Clean Cuts (now public) && (LAT frame theta) < 65º && (Earth zenith angle) <105º && abs(LAT Rocking angle) < 52º
- Removed 1087 point sources, using 1FGL Catalog (1451 sources total).

✓ Cut Radius @ PSF 68% containment

✓ 6 point sources within a 2 deg by 2 deg square at the GC are not removed.

✓ Removes ~10% of photons

Region of the Sky Used in Analysis

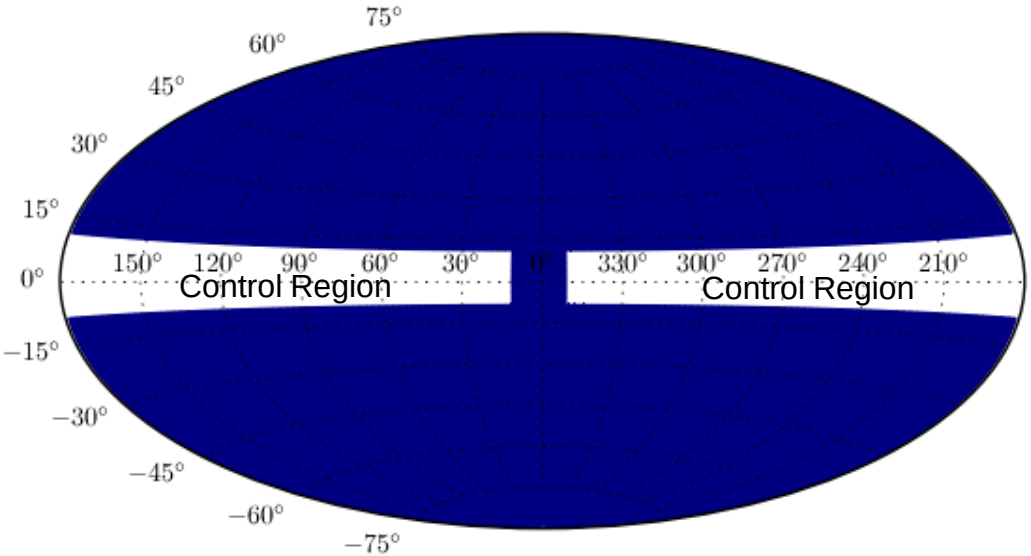

- **This work is largely based on the thesis of Y. Edmonds of SLAC, Stanford University. She defended in early March.**

Fermi LAT Inclusive Photon Spectrum from ROI 4.8 – 264 GeV

- Inclusive Photon Spectrum is featureless power-law, index ~2.44 (13 < E < 264 GeV)
- Estimate background from charged particles to be < 5% for E > 100 GeV based on results from LAT Extragalactic Background results (Abdo et al. 2010), and MC of CR background spectrum yielding index ~ 2.6 after cuts (compared to our measured index of 2.44 for γs). No additional CR subtraction is made based on this estimate at this time.

E^2 x flux [$GeVcm^{-2}s^{-1}sr^{-1}$]
P6V3 dataclean class

± 20 % Systematic error on effective area

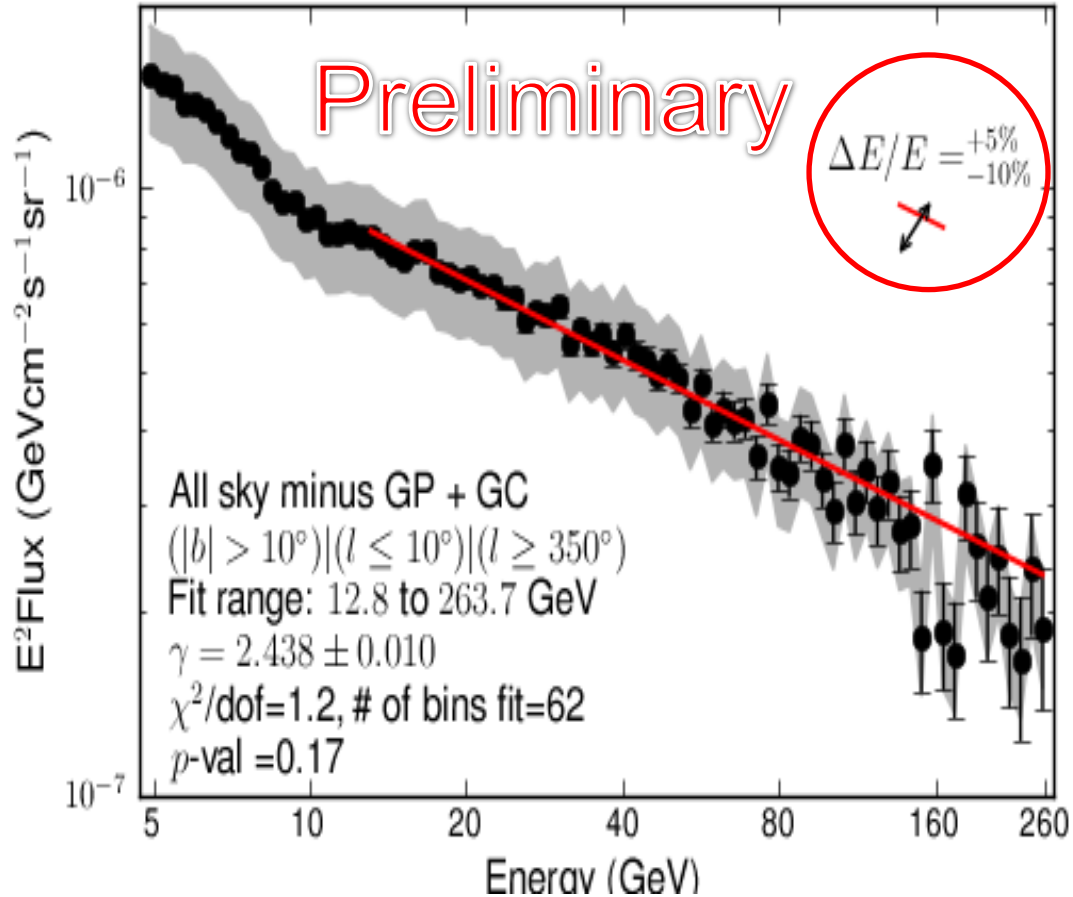

Challenges some final state radiation models

"Decaying Dark Matter as a Probe of Unification and TeV Spectroscopy", Arvanitaki, A., et al., Phys.Rev.D80:055011,2009.

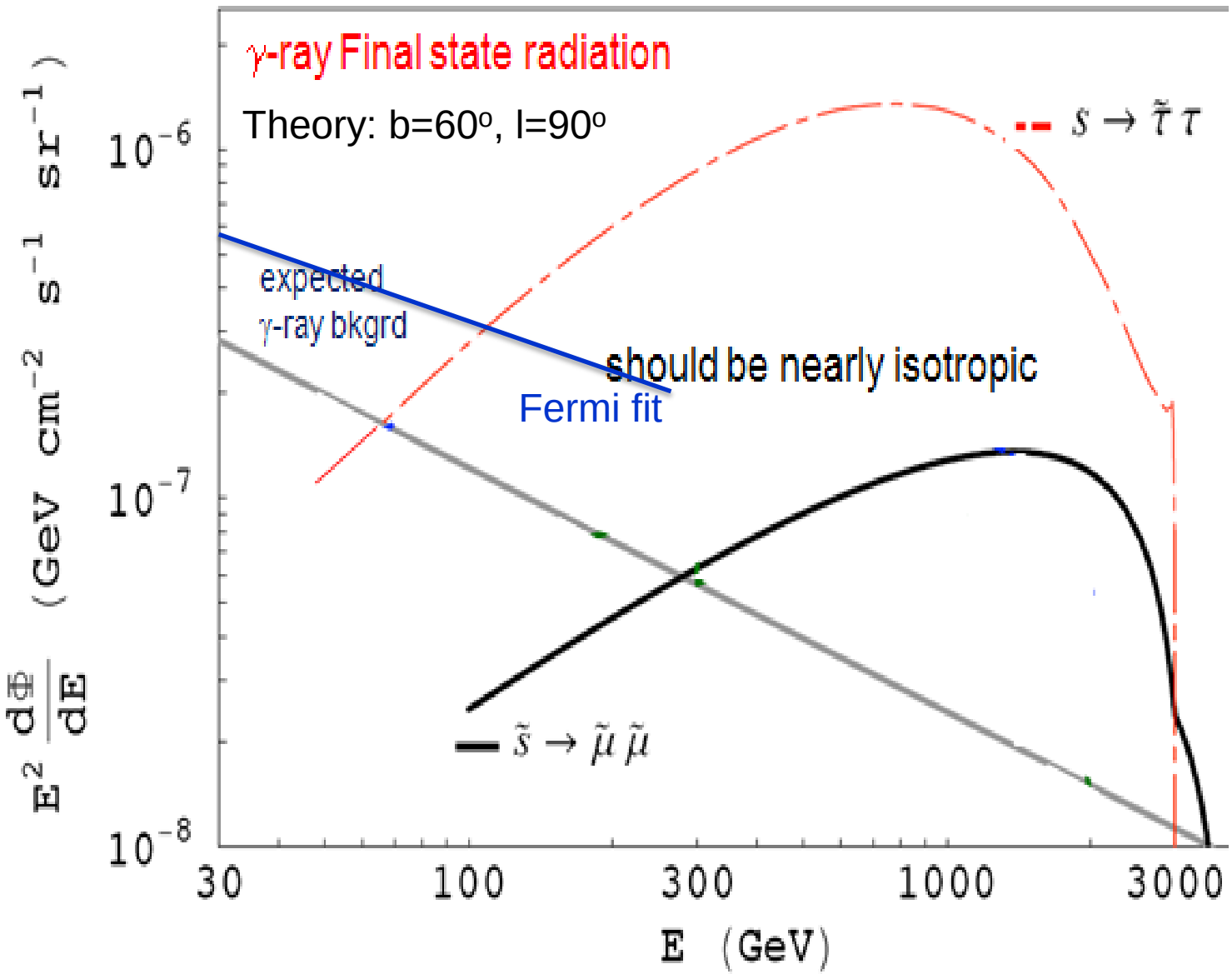

Search for Spectral Lines

- The shape of the line is determined by the Fermi LAT resolution function for the profile energy determined via MC and checked with beam test results.
  - Resolution (68% containment) = - 8% + 5% @ 7 GeV
  - Resolution (68% containment) = -10% +10% @ 200 GeV
  - Composite likelihood fits signal + background *S(E)* = signal pdf, *B(E)* = background pdf = power law, *f* = signal fraction
  - *f* and Γ free, *f* ≥0 constraint

$$L = \prod_{i=0}^{N} f \cdot S(E_i) + (1 - f) \cdot B(E_i, \Gamma)$$

- Fitting ranges in search are ± 4σ wide on a grid of energies: 7,10,15,20,30,40,50,…,200. (Control "look-elsewhere" effect.)
  - The fitting ranges overlap significantly
  - LAT team analysis shows a systematic effect that gives an enhanced signal at ~ 7 GeV that is mainly the result of analysis data cut in P6V3 ("CTBCORE"). This is being changed in future releases. Beware the smoking gun in P6V3! Solved with pass 7 to be released this year.
    - "CTBCORE" is a high level cut variable that influences the quality of the γ directional information.
  - The LAT team reports no lines observed, and gives upper limits. No detection at 95% CL.

Fermi LAT 23 Month Line search results
Flux Upper Limits, 7 GeV – 200 GeV

- ± 20 % overall scale systematic error (+20 % systematic for UL).
- Additional systematic on spectral structures with LAT resolution for E < 13.2 GeV of s/bg ~ 1%. 7 and 10 GeV bins use a modified event selection to reduce the systematic uncertainty associated with public IRFs.
- For E > 12 GeV no indication of a spectral structure systematic effect is seen.

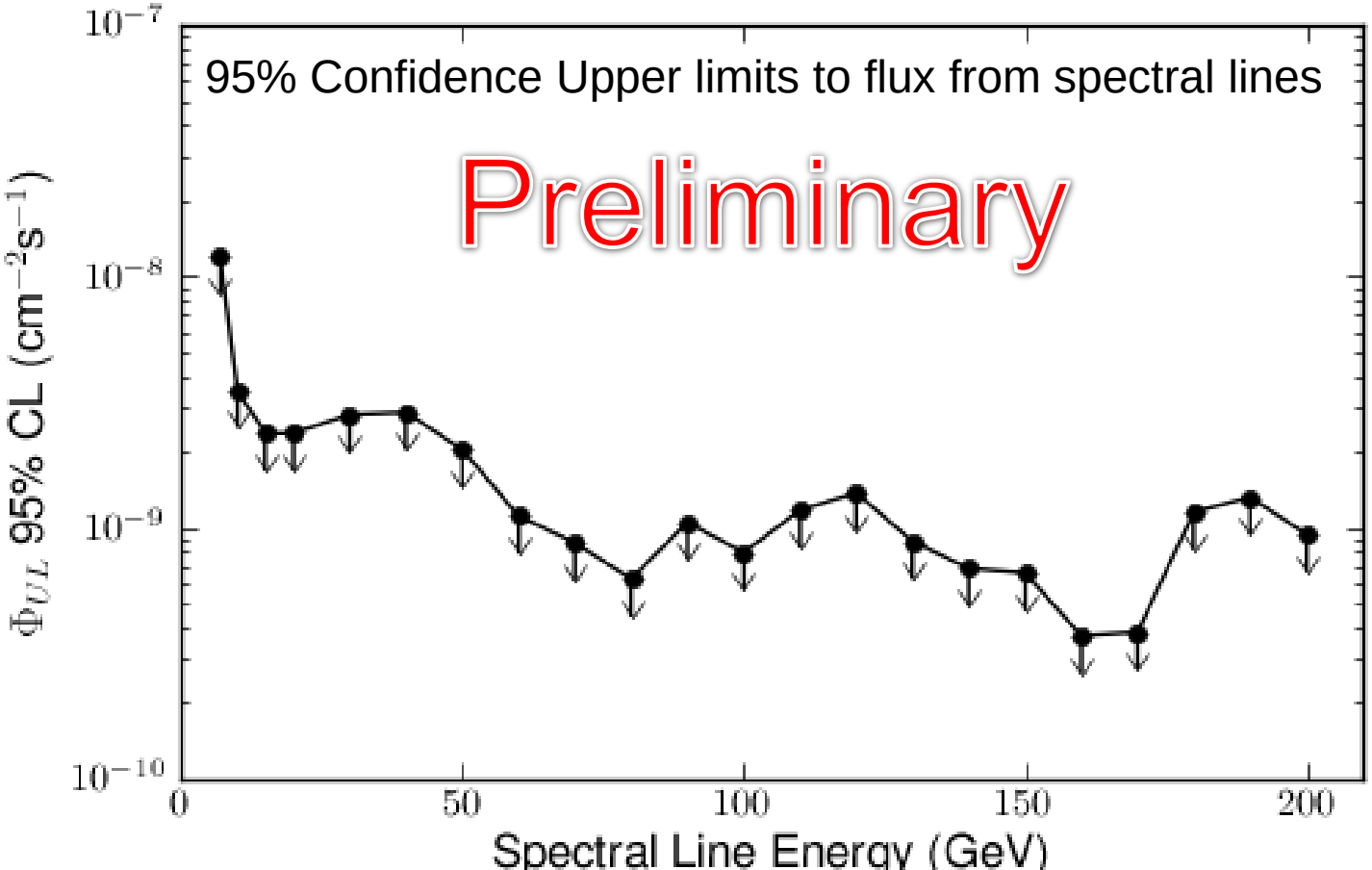

Fermi LAT 23 Month
γγ-Cross-section upper limits
7 GeV – 200 GeV

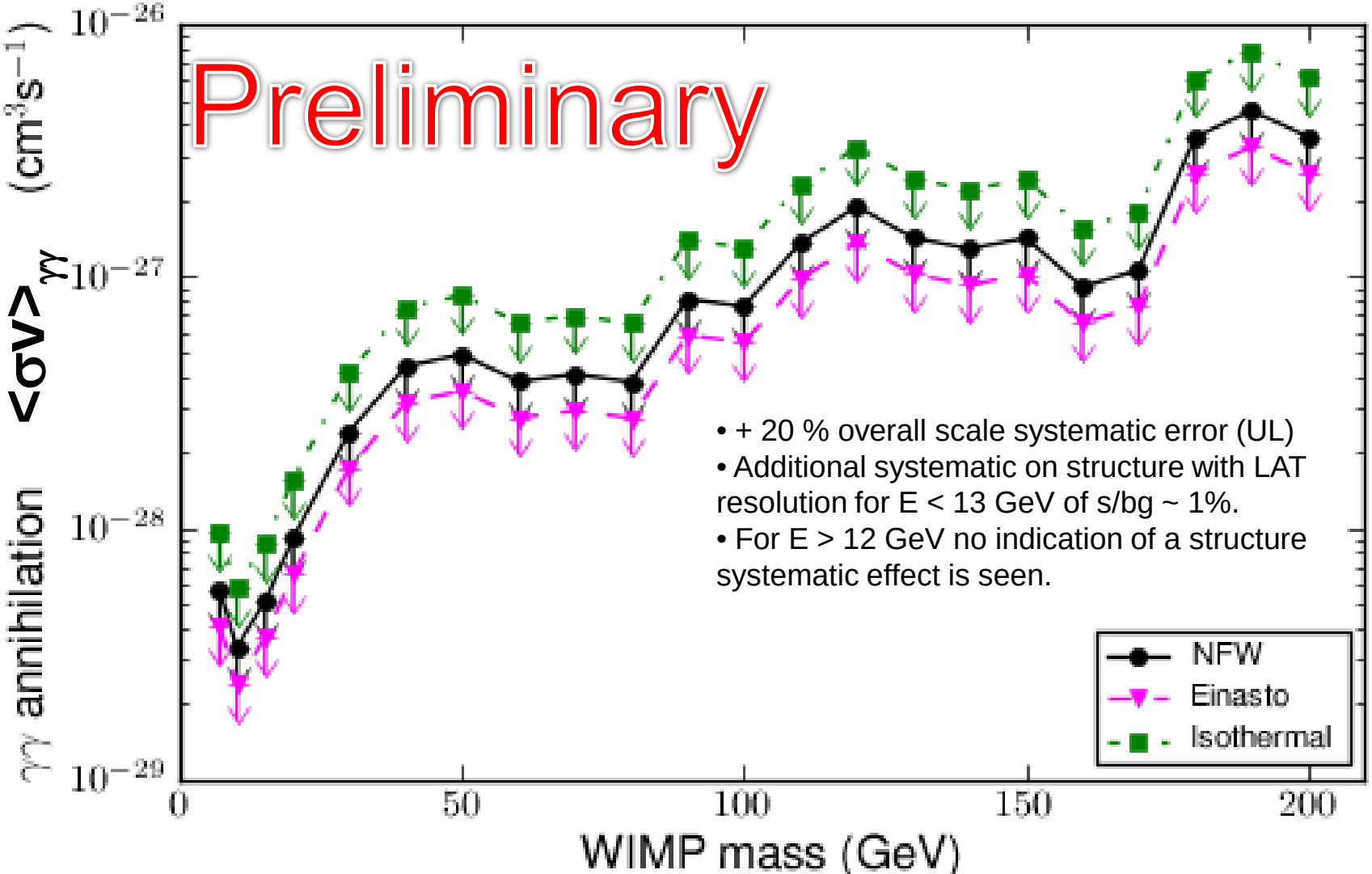

Fermi LAT 23 Month
γZ-Cross-section limits
7 GeV – 200 GeV

- + 20 % overall scale systematic error (UL)
- Additional systematic on structure with LAT resolution for E < 13 GeV of s/bg ~ 1%.
- For E > 12 GeV no indication of a structure systematic effect is seen.

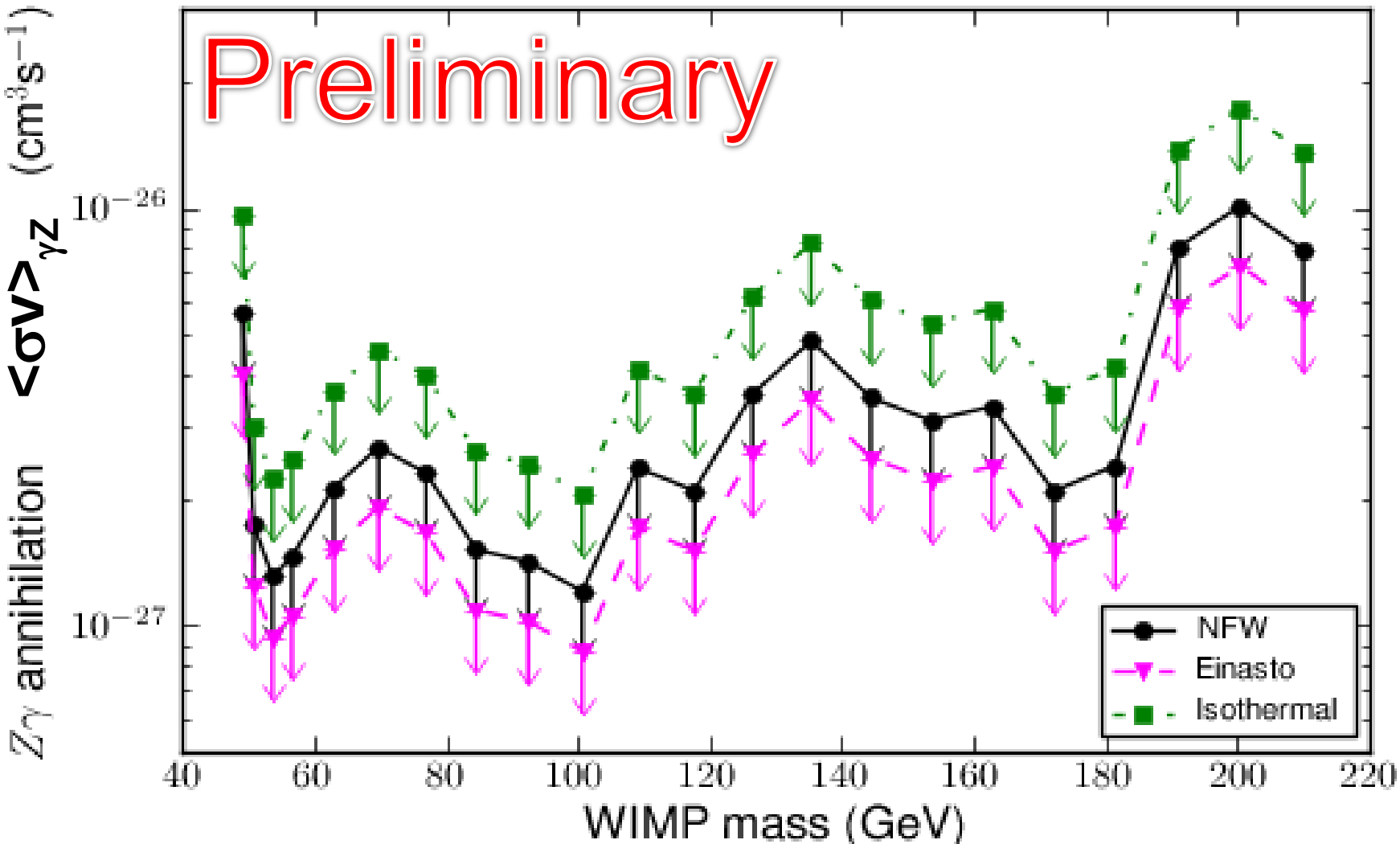

Fermi LAT 23 Month γZ-Cross-section limits 7 GeV – 200 GeV

- +20 % overall scale systematic error (UL)
- Additional systematic on structure with LAT resolution for E < 13 GeV of s/bg ~ 1%.
- For E > 12 GeV no indication of a structure systematic effect is seen.

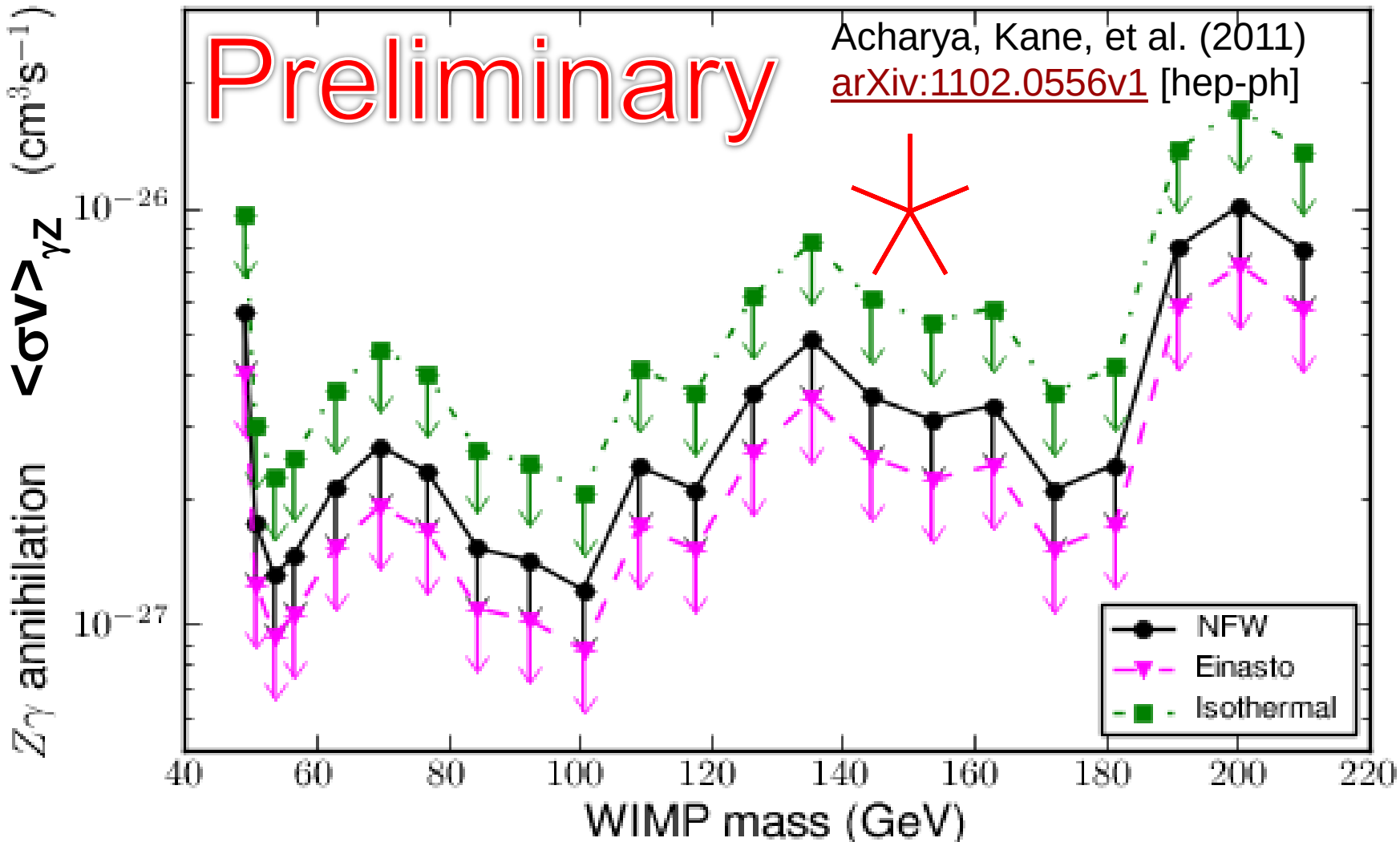

Gamma Ray Line Constraints on Effective Theories of Dark Matter

Jessica Goodman, et al. arXiv:1009.0008v2 [hep-ph] 18 Dec 2010

Similar to early days of the study of weak interactions.

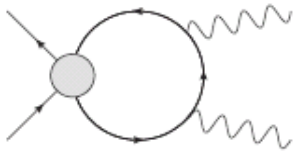

FIG. 1: Representative Feynman diagram for the loop level annihilation of two DM particles χ to a photon and a second vector boson, either another photon or a Z boson, through an operator coupling the DM to SM quarks (represented as the shaded circle).

D for Dirac fermion, M for Majorana, C for complex scalar, and R for real scalar and the number specifies the particular operator belonging to a given WIMP spin. Within each family, the earlier numbers refer to coupling to quark scalar bilinears (D1-4, M1-4, C1-2, and R1-2), the middle numbers to quark vector bilinears (D5-8, M5-6, and C3-4) and quark tensor bilinears (D9-10) and the largest numbers to coupling to gluons (D11-14, M7-10, C5-6, and R3-4). The WIMP electric and magnetic dipole moment operators are labeled D15 and D16.

Name	Operator	Coefficient
D1	$\bar{\chi}\chi\bar{q}q$	m_q/M_*^3
D2	$\bar{\chi}\gamma^5\chi\bar{q}q$	im_q/M_*^3
D3	$\bar{\chi}\chi\bar{q}\gamma^5 q$	im_q/M_*^3
D4	$\bar{\chi}\gamma^5\chi\bar{q}\gamma^5 q$	m_q/M_*^3
D5	$\bar{\chi}\gamma^\mu\chi\bar{q}\gamma_\mu q$	$1/M_*^2$
D6	$\bar{\chi}\gamma^\mu\gamma^5\chi\bar{q}\gamma_\mu q$	$1/M_*^2$
D7	$\bar{\chi}\gamma^\mu\chi\bar{q}\gamma_\mu\gamma^5 q$	$1/M_*^2$
D8	$\bar{\chi}\gamma^\mu\gamma^5\chi\bar{q}\gamma_\mu\gamma^5 q$	$1/M_*^2$
D9	$\bar{\chi}\sigma^{\mu\nu}\chi\bar{q}\sigma_{\mu\nu}q$	$1/M_*^2$
D10	$\bar{\chi}\sigma_{\mu\nu}\gamma^5\chi\bar{q}\sigma_{\mu\nu}q$	i/M_*^2
D11	$\bar{\chi}\chi G_{\mu\nu}G^{\mu\nu}$	$\alpha_s/4M_*^3$
D12	$\bar{\chi}\gamma^5\chi G_{\mu\nu}G^{\mu\nu}$	$i\alpha_s/4M_*^3$
D13	$\bar{\chi}\chi G_{\mu\nu}\tilde{G}^{\mu\nu}$	$i\alpha_s/4M_*^3$
D14	$\bar{\chi}\gamma^5\chi G_{\mu\nu}\tilde{G}^{\mu\nu}$	$\alpha_s/4M_*^3$
D15	$\bar{\chi}\sigma^{\mu\nu}\chi F_{\mu\nu}$	M
D16	$\bar{\chi}\sigma_{\mu\nu}\gamma^5\chi F_{\mu\nu}$	D
M1	$\bar{\chi}\chi\bar{q}q$	$m_q/2M_*^3$
M2	$\bar{\chi}\gamma^5\chi\bar{q}q$	$im_q/2M_*^3$

Name	Operator	Coefficient
M3	$\bar{\chi}\chi\bar{q}\gamma^5 q$	$im_q/2M_*^3$
M4	$\bar{\chi}\gamma^5\chi\bar{q}\gamma^5 q$	$m_q/2M_*^3$
M5	$\bar{\chi}\gamma^\mu\gamma^5\chi\bar{q}\gamma_\mu q$	$1/2M_*^2$
M6	$\bar{\chi}\gamma^\mu\gamma^5\chi\bar{q}\gamma_\mu\gamma^5 q$	$1/2M_*^2$
M7	$\bar{\chi}\chi G_{\mu\nu}G^{\mu\nu}$	$\alpha_s/8M_*^3$
M8	$\bar{\chi}\gamma^5\chi G_{\mu\nu}G^{\mu\nu}$	$i\alpha_s/8M_*^3$
M9	$\bar{\chi}\chi G_{\mu\nu}\tilde{G}^{\mu\nu}$	$i\alpha_s/8M_*^3$
M10	$\bar{\chi}\gamma^5\chi G_{\mu\nu}\tilde{G}^{\mu\nu}$	$\alpha_s/8M_*^3$
C1	$\chi^\dagger\chi\bar{q}q$	m_q/M_*^2
C2	$\chi^\dagger\chi\bar{q}\gamma^5 q$	im_q/M_*^2
C3	$\chi^\dagger\partial_\mu\chi\bar{q}\gamma^\mu q$	$1/M_*^2$
C4	$\chi^\dagger\partial_\mu\chi\bar{q}\gamma^\mu\gamma^5 q$	$1/M_*^2$
C5	$\chi^\dagger\chi G_{\mu\nu}G^{\mu\nu}$	$\alpha_s/4M_*^2$
C6	$\chi^\dagger\chi G_{\mu\nu}\tilde{G}^{\mu\nu}$	$i\alpha_s/4M_*^2$
R1	$\chi^2\bar{q}q$	$m_q/2M_*^2$
R2	$\chi^2\bar{q}\gamma^5 q$	$im_q/2M_*^2$
R3	$\chi^2 G_{\mu\nu}G^{\mu\nu}$	$\alpha_s/8M_*^2$
R4	$\chi^2 G_{\mu\nu}\tilde{G}^{\mu\nu}$	$i\alpha_s/8M_*^2$

TABLE I: Operators coupling WIMPs to SM particles. The operator names beginning with D, M, C, R apply to WIMPs that are Dirac fermions, Majorana fermions, complex scalars or real scalars respectively.

Gamma Ray Line Constraints on Effective Theories of Dark Matter

Jessica Goodman, et al. arXiv:1009.0008v2 [hep-ph] 18 Dec 2010 Fermi data points from **PRL 11 months of data.**

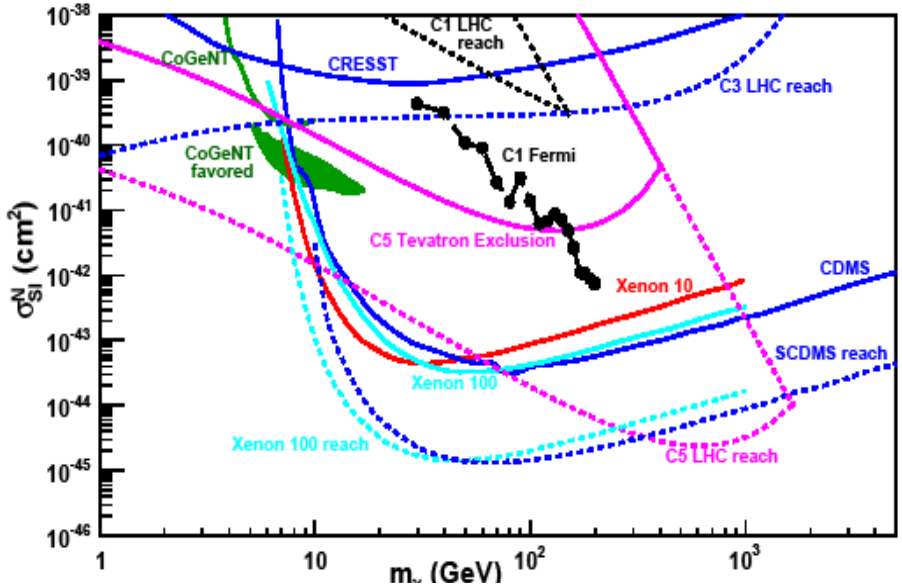

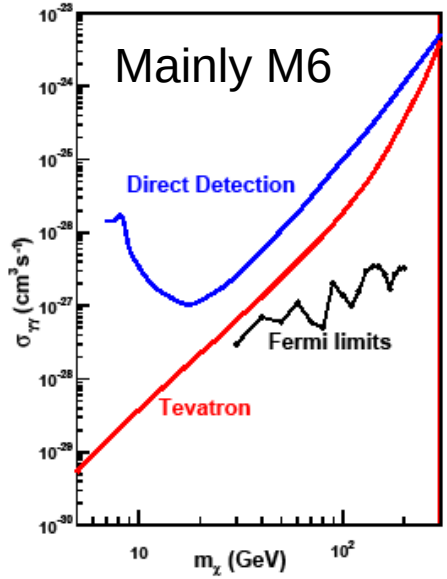

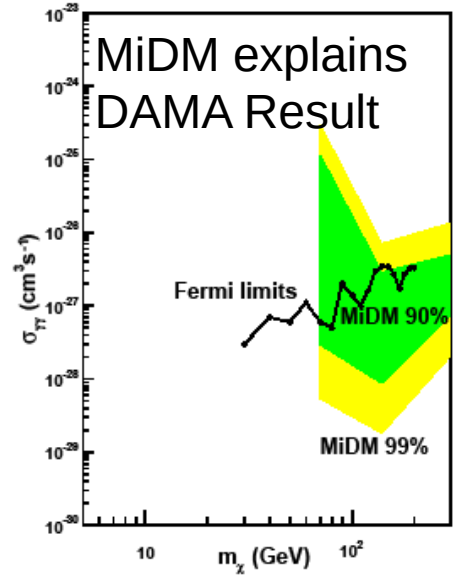

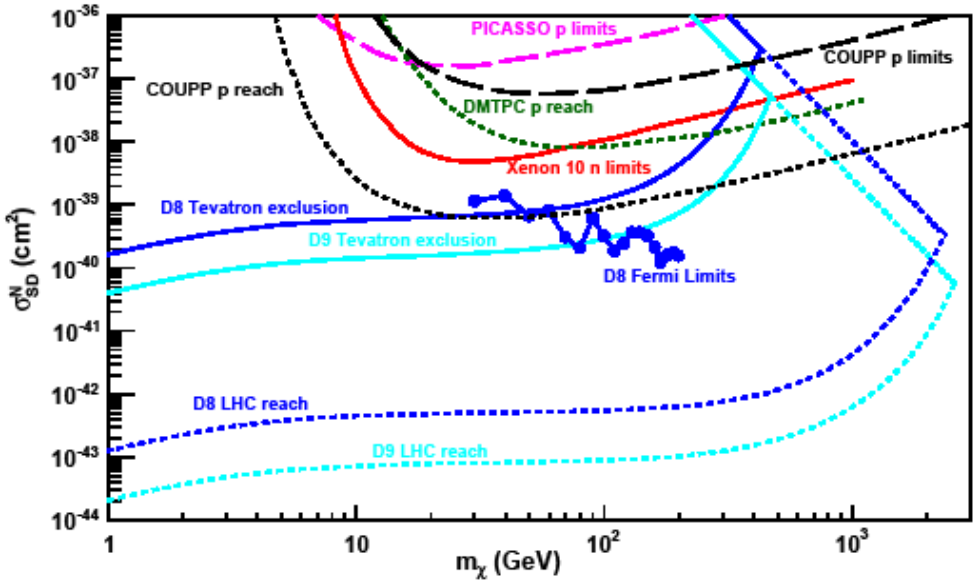

Plots for the PRL line search, mapped into direct detection parameter space assuming an NFW profile. The two plots on left are for a scalar WIMP. The top right indirect detection plots are for a Majorana WIMP. (T. Tait Private communication)

The Fermi LAT Search for Large Extra Dimensions

- Set limits on the size and scale of large extra dimensions (LED), based on theory proposed by Arkani-Hamed, Dimopoulos, and Dvali (ADD) (1998, *Phys. Lett. B* **436**: 263–272)
- ADD postulated the existence of large extra dimensions as an explanation for the difference between the gravitational scale to electroweak scale (the hierarchy problem).
  - Planck scale: $M_{P,4}$ = 1.22×10^{16} TeV
    - determined by gravitational coupling
  - Electroweak scale: M_{EW} ~ 1 TeV

$$M_{P,4} = \sqrt{\frac{\hbar c}{G_N}}; \quad \bar{M}_{P,4} = \frac{M_{P,4}}{\sqrt{8\pi}} = 2.4\times10^{15} \text{ TeV}$$

(reduced Planck mass)

- For a given number of extra dimensions *n*, they considered compactified dimensions of the <u>same size</u>, R, in this model.
- Due to the presence of extra dimensions, the effective Planck mass in n+4 dimensions, $M_{P,n+4}$ would be brought closer to the electroweak scale (~ 1 TeV).

$$\boxed{\bar{M}_{P,4}^{2} = M_{P,n+4}^{n+2} R^{n}}$$

(natural units)

- In this scenario, gravity in 4 dimensions is weak because it is diluted in a large space. Standard Model fields DO NOT propagate in the extra dimensions.

Limits on LED from Neutron Stars

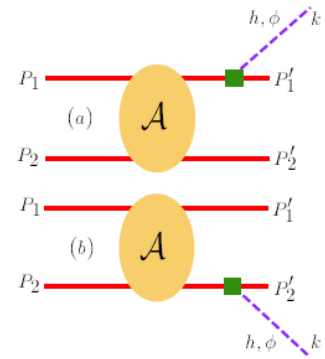

- In the LED model by ADD, Kaluza-Klein (KK) gravitons (h) are produced via nucleon-nucleon gravi-bremsstrahlung in supernova cores (involves scattering process of nucleons)

$$NN \longrightarrow NNh$$

- h particles have masses ~ 100 MeV, lifetimes of ~10^9 yr, and decay into photons: $h \longrightarrow \gamma\gamma$

- The first astrophysical bounds on LED were placed indirectly from SN1987A
  - based on neutrino signal precluding too much energy loss into the KK gravitons' channel

- Restrictive limits on the size of extra dimensions can be placed from neutron star γ–ray emission originating from trapped *h* graviton decay.
  - See Hannestad and Raffelt, 2003, *Phys. Rev. D* **67** 125008
  - For n< 4, more stringent limits than can be probed by signatures of LED at colliders, about the same for n=4

Limits on LED from Neutron Stars

- In this model, neutron stars (NS) will shine in ~100 MeV γ-rays.
  - Previous results have no corrections for orbit, decay and absorption in B field.
  - Hannestad and, Raffelt (2003): used EGRET point source sensitivity as basis for results.
  - Cassé ,Paul, Bertone, Sigl (2004): averaged over a population of ~10^9 NS in the galactic disk using EGRET data.

The Pulsing Gamma-ray Sky As of December 2010

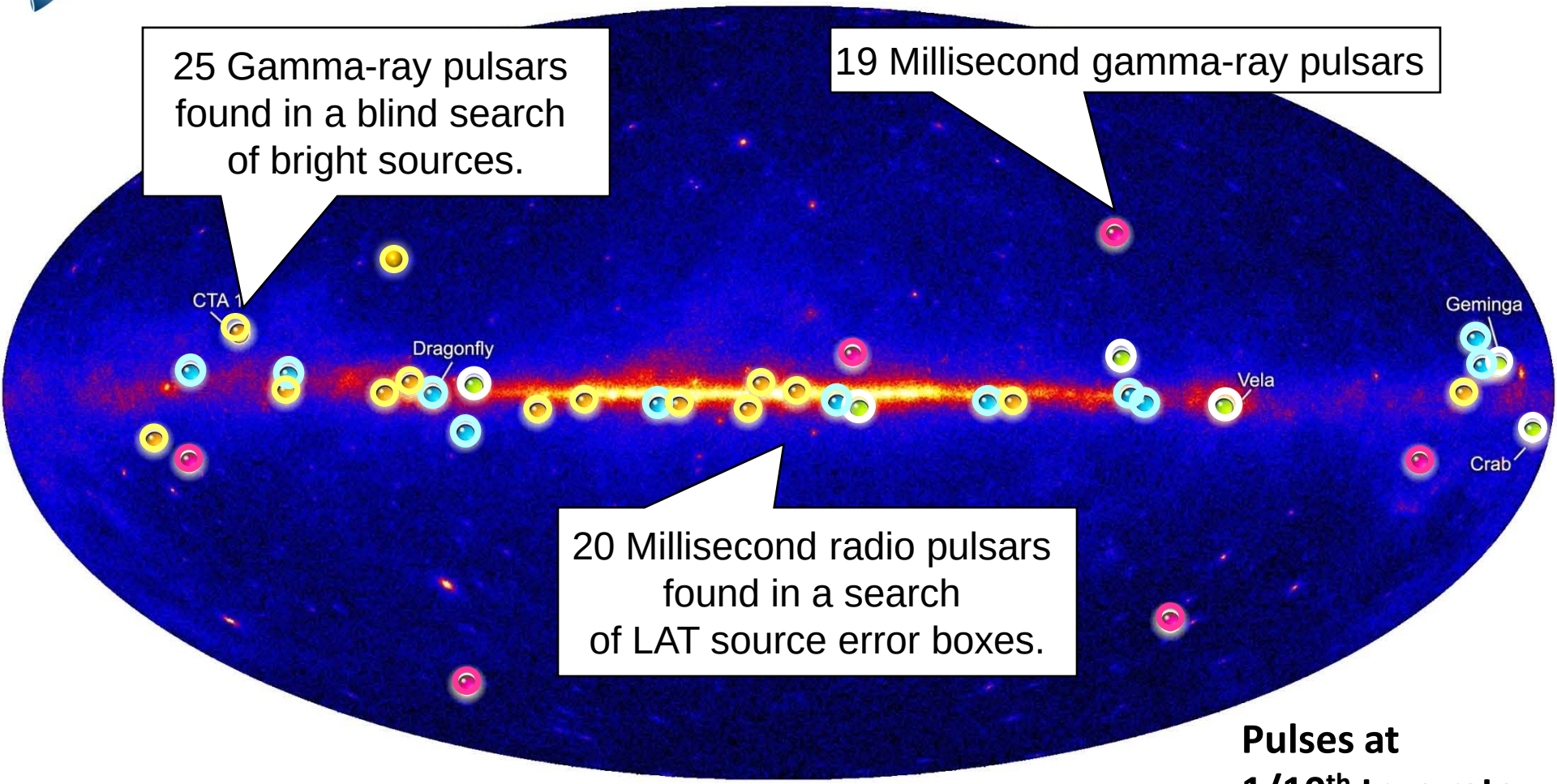

Pulses at 1/10th true rate

- New pulsars discovered in a blind search
- Millisecond radio pulsars
- Young radio pulsars
- Pulsars seen by Compton Observatory EGRET instrument

Fermi Pulsar Detections

> 86 γ-ray pulsars are now known.

Data on Candidate Pulsar Sources

Criteria for selecting pulsar sources:

- t_{age} < 2x10^8 yr (not too old)
- B_{surf} < 3x10^{13} gauss (not too high field)
- $|b|$ > 15° (avoid galactic plane)
- Dist. < 0.4 kpc (sensitivity)
- Not Fermi-LAT source in 1FGL (gives bad limit)

•This work is largely based on the thesis of Bijan Berenji of SLAC, Stanford University. He is defending in mid-April (and looking for a post doc job).

name	RA (°)	Dec (°)	ℓ (°)	b (°)	Period (s)	d (kpc)	Age (yr)	B_{surf} (G)
RXJ1856-3754	284.1	-37.9	358.6	-17.2	7.05	0.16	3.76E6	1.47E1
J0108-1431	17.0	-14.3	140.9	-76.8	0.808	0.24	1.66E8	2.52E1
J0953+0755	148.2	7.9	228.9	43.7	0.25	0.26	1.75E7	2.44E1
J0630-2834	97.7	-28.5	236.9	-16.7	1.24	0.33	2.77E6	3.01E1
J1136+1551	174.0	15.8	241.9	69.2	1.19	0.36	5.04E6	2.13E1
J0826+2637	126.7	26.6	196.9	31.7	0.53	0.36	4.92E6	9.64E1

(Data obtained from ATNF Catalog, NASA HEASARC mirror site.)

Fermi LAT Lower Limits on Unification Scale

- 95% CL Lower Limits on the (n+4)-dimensional Planck Scale (TeV units), $M_D \equiv M_{P,n+4}$
- Better than past collider limits (DØ,CDF,LEP) for n <5, LHC for n < 4
- Interpretation:
  - if unification occurs at around a TeV, n > 4 LED are favored **from our results**
  - If unification occurs for n = 2 or 3, the compactification topology is more complicated than a torus (e.g., warping, different sizes for different dimensions)

n	J1856-3754	J0108-1431	J0953+0755	J1136+1551	J0630-2834	J0826+2637	Combined	DØ	CDF	LEP	CMS (LHC)
2	**210**	**91**	**140**	**130**	**130**	**120**	**230**	**2.09**	**1.40**	**1.60**	**1.8**
3	**14**	**7.6**	**10**	**10**	**10**	**9.0**	**15**	**1.94**	**1.15**	**1.20**	**3.4**
4	**2.3**	**1.4**	**1.8**	**1.7**	**1.7**	**1.5**	**2.5**	**1.62**	**1.04**	**0.94**	**3.3**
5	0.63	0.41	0.50	0.50	0.46	0.44	0.66	1.46	0.98	0.77	3.2
6	0.24	0.16	0.19	0.19	0.17	0.17	0.24	1.36	0.94	0.66	3.0
7	0.11	0.078	0.091	0.091	0.081	0.080	0.11	1.29	-	-	

Preliminary

LEP (2004): http://lepexotica.web.cern.ch/LEPEXOTICA
DØ (2008): http://arxiv.org/abs/0809.2813v1 (1.05 fb^{-1}, diphoton, dilepton modes)
CDF (2008): http://arxiv.org/abs/0807.0645v1
ATLAS/CMS (2011) : arXiv:1101.4919v1 [hep-ph]

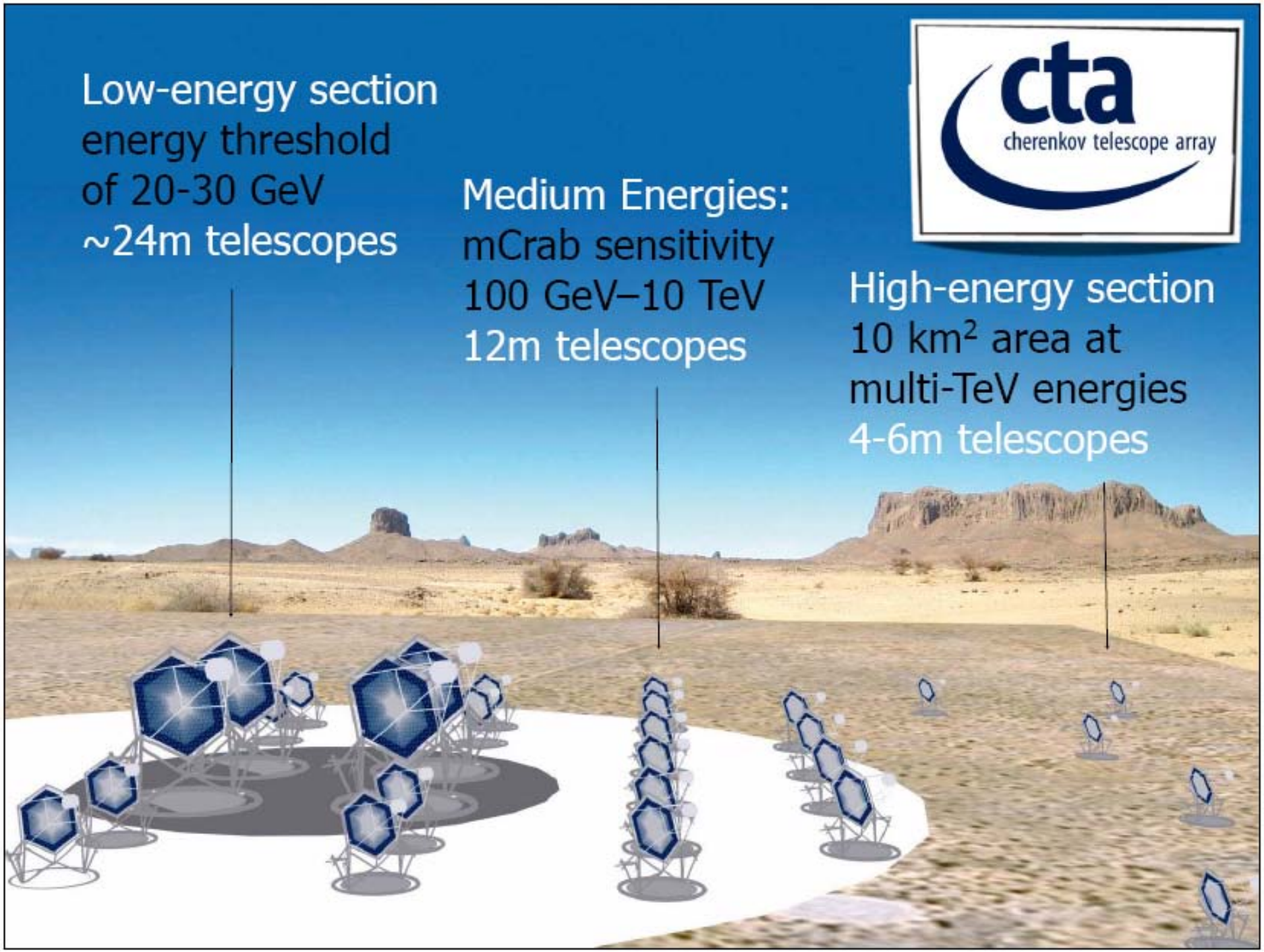
Low-energy section
energy threshold
of 20-30 GeV
~24m telescopes
Medium Energies:
mCrab sensitivity
100 GeV–10 TeV
12m telescopes
High-energy section
10 km² area at
multi-TeV energies
4-6m telescopes
cta
cherenkov telescope array

Example: Sensitivities for WIMP detection

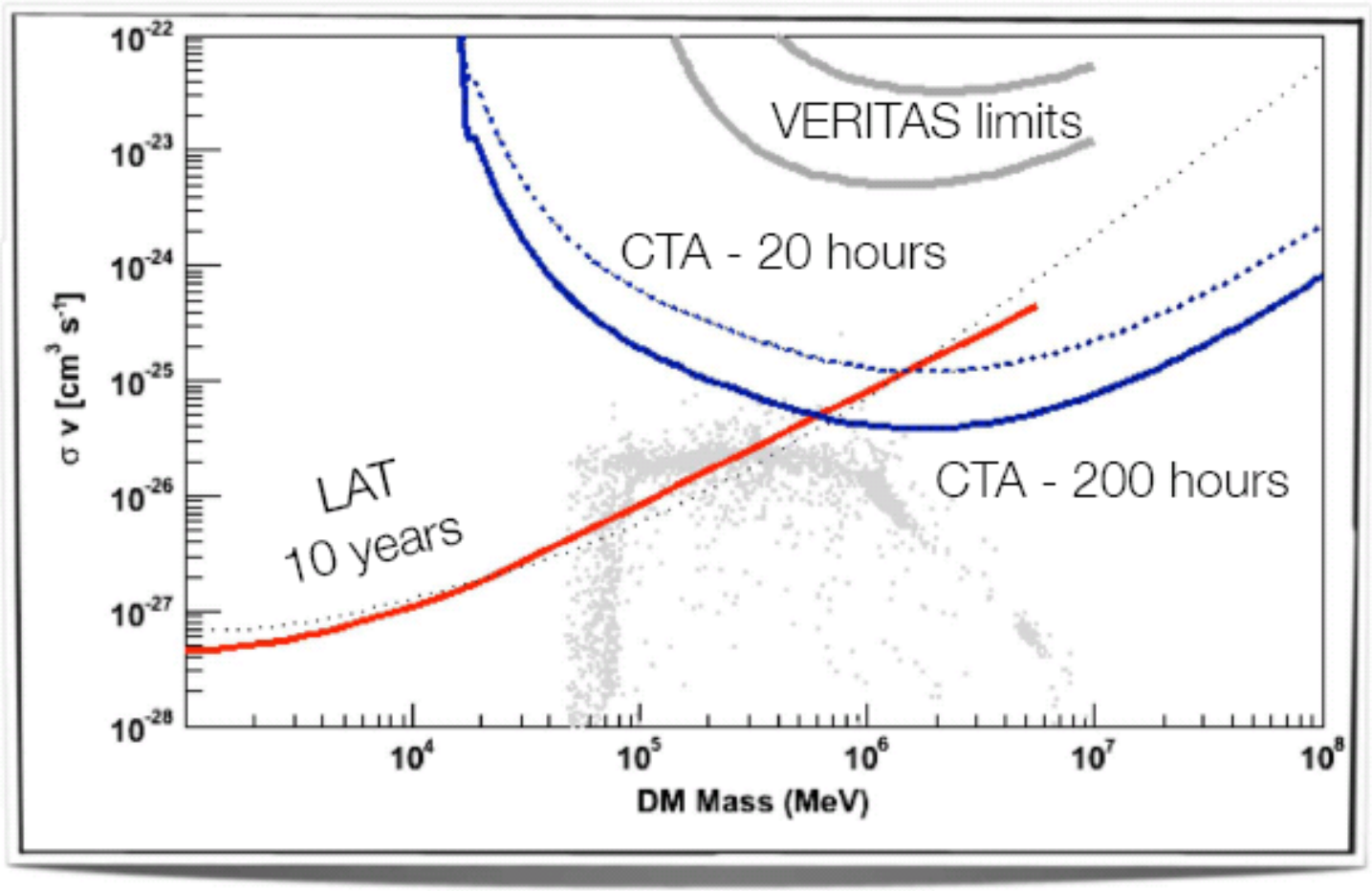

- Cross-over mass for DM wimp at ~500 GeV (for J = 10^{14} Mo^{-2} kpc^{-5})

CTA Collaboration Estimate

Complementarity direct and indirect detection methods

Direct detection (scattering)

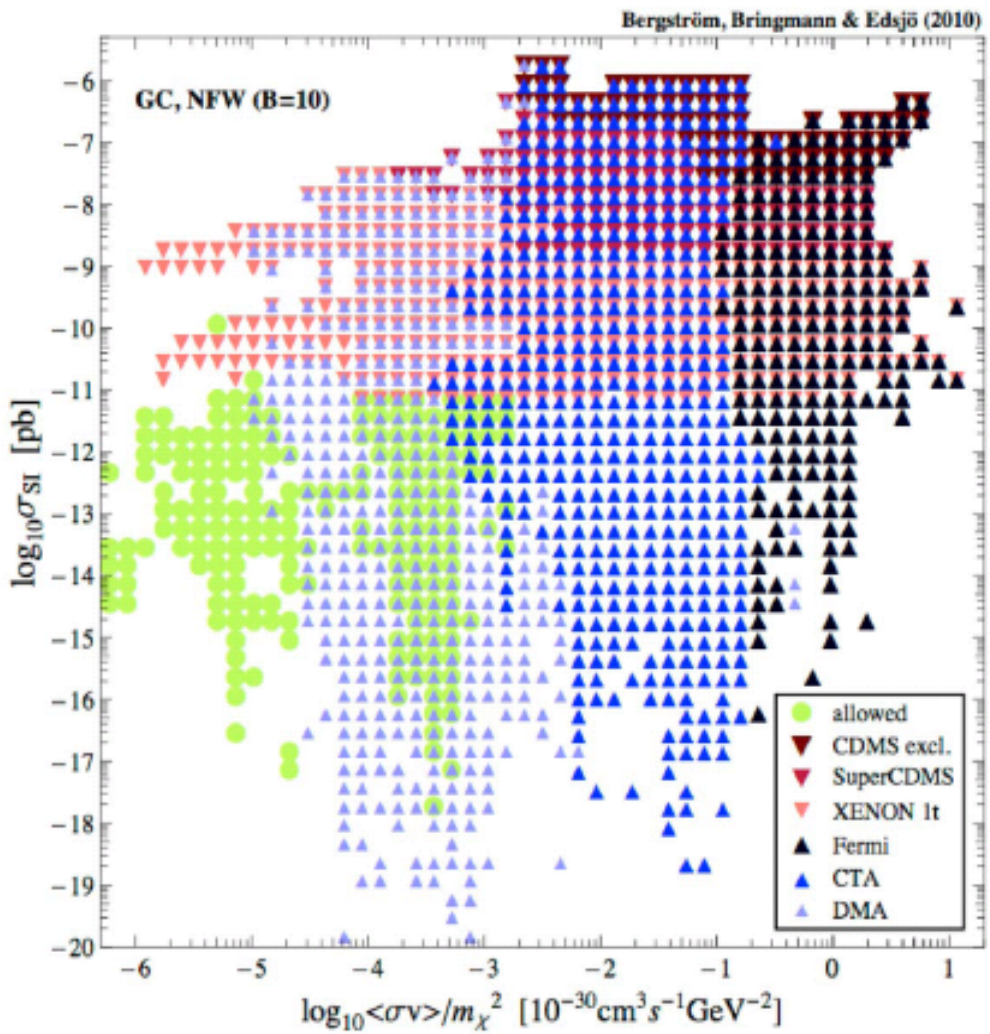

MSSM / mSUGRA models

Dark Matter Array (DMA)
See Bergstrom et al. (2010)
CTA at high altitude
(10 GeV threshold).

Indirect detection (annihilation γ's)

Conclusions I

- No discovery... however promising constraints on the nature of DM have been placed.
  - Our knowledge of the astrophysical background is uncertain. This is currently a big limitation in particular for the Galactic center and the Galactic halo which otherwise have huge potential in terms of discovery or setting constraints. It requires a dedicated effort.
  - An another example of better understanding is our study of Fermi pulsar SEDs and how they can fake WIMP decay at lower mass (coming soon).
- In addition, better understanding of the dark matter density distribution is essential in interpreting observations.
- Some analyses will further benefit from multi-wavelength observations (e.g. dSph and DM satellites.) And if a signal is observed elsewhere (e.g. LHC) it's likely to make our job easier!
- If a signal is found, indirect detection will provide invaluable information on the distribution of dark matter and will offer a glimpse into the thermal relic hypothesis by measuring the annihilation cross section

Conclusions II

- Fermi is a 5 year mission, with a goal of 10 years.
- Even with current limits from Fermi γ-ray observations, Fermi LAT Collaboration results are challenging interesting parts of the theoretical phase space.
  - This is particularly the case for DM models that sprang-up to explain the ATIC, Pamela, and Fermi electron and positron results.
  - The photon line limits have a broader significance beyond specific models using an effective field theory formalism. Easy comparison with direct detection and accelerator DM results.
  - The limits on the search for ELD have excluded up to d=3 for the ADD model.
- Data analysis: Pass 7 will be a significant improvement over the current public data, Pass 6, and will be released this year. Pass 8 is in the works!
- For the longer term future CTA, perhaps a special indirect dark matter tuned version, DMA, has promise to dramatically improve the search space.

Thank You!

Extra Slides

LAT Collaboration

- France
  - CNRS/IN2P3, CEA/Saclay
- Italy
  - INFN, ASI, INAF
- Japan
  - Hiroshima University
  - ISAS/JAXA
  - RIKEN
  - Tokyo Institute of Technology
- Sweden
  - Royal Institute of Technology (KTH)
  - Stockholm University
- United States
  - Stanford University (SLAC and HEPL/Physics)
  - University of California, Santa Cruz - Santa Cruz Institute for Particle Physics
  - Goddard Space Flight Center
  - Naval Research Laboratory
  - Sonoma State University
  - The Ohio State University
  - University of Washington

PI: Peter Michelson
(Stanford)

~400 Scientific Members (including 96 Affiliated Scientists, plus 68 Postdocs and 105 Students)

Cooperation between NASA and DOE, with key international contributions from France, Italy, Japan and Sweden.

Project managed at SLAC.

25.6 Degree Orbit

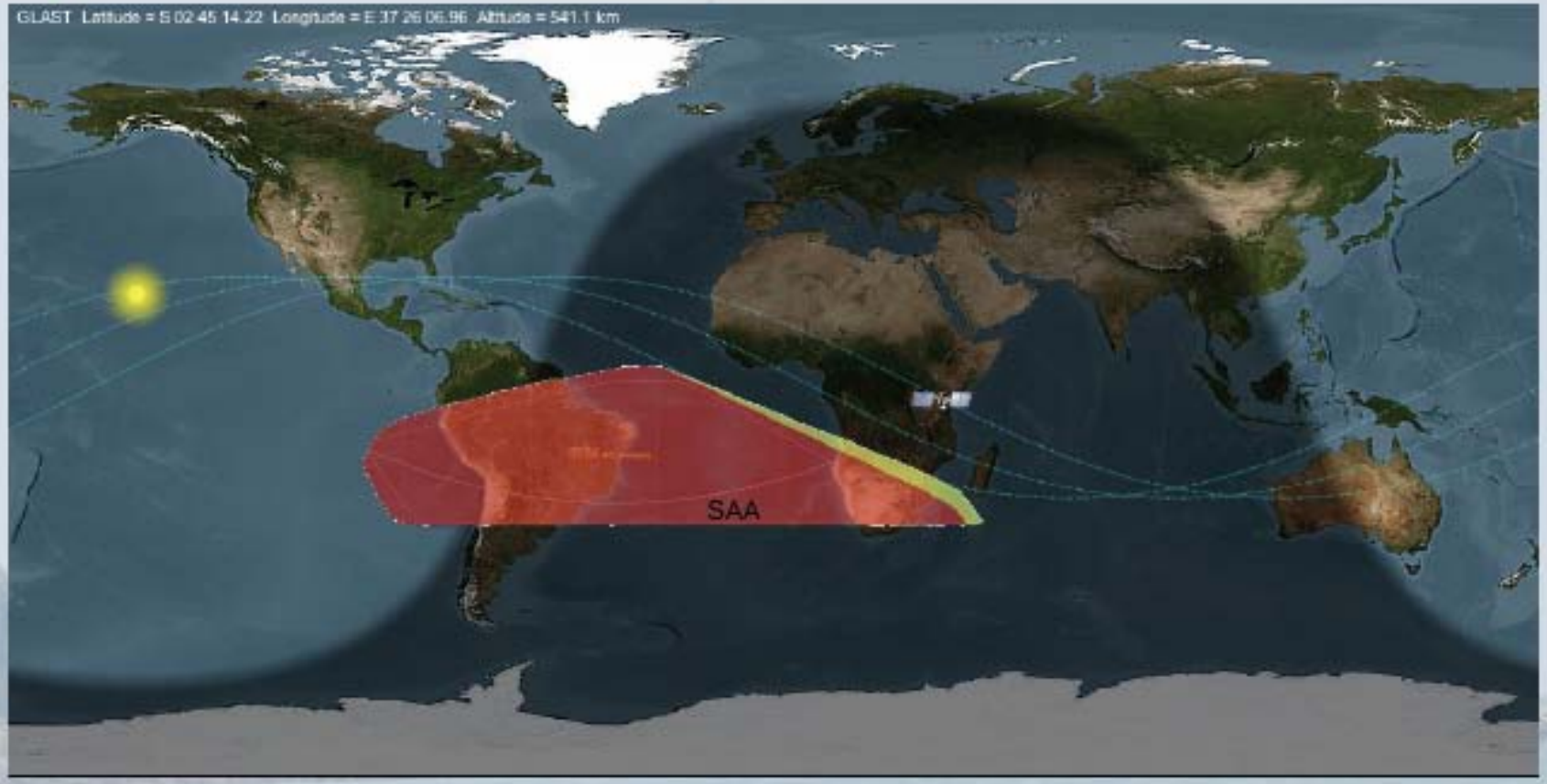

http://observatory.tamu.edu:8080/Trakker/

Circular orbit, 565 km altitude (96 min period), 25.6 deg inclination

The extragalactic background diffuse emission (EGB)

has an isotropic distribution on the sky, and is considered to be the superposition of different classes of unresolved sources (AGNs, star-forming galaxies, GRBs) and genuinely diffuse processes like the interaction of ultra-high energy cosmic rays with the extragalactic background light, structure formation shocks, and potential contributions from the decay or annihilation of dark matter.

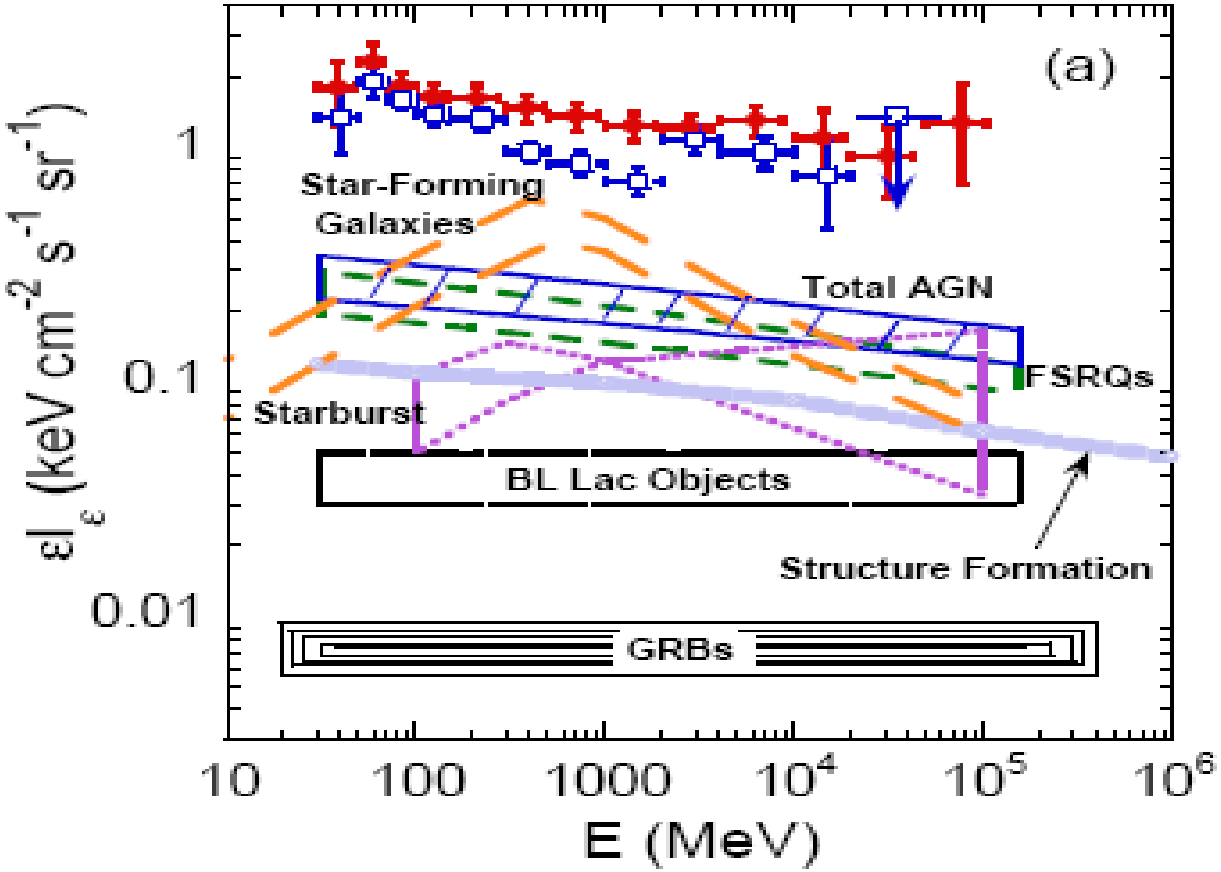

Compilation of predictions of EGB contributions from different unresolved source classes and diffuse processes in comparison to the EGB measured by EGRET. This figure is adopted from Dermer 2007 (pre Fermi Launch prediction).

Fermi Population Paper Some Details Abdo, A. A., et al. 2010, ApJ. 720, 435

Comments below are from Marco Ajello, one of the lead authors on this paper:

- In our paper, the hypothesis that blazars can be represented by a power-law spectrum is discussed and showed not to introduce a strong bias. To show this we derived 3 independent logN-logS distributions in 3 contiguous energy bands (0.1-1 GeV, 1-10 GeV and 10-100 GeV). These can be integrated to derive the contribution to the background in those bands and this is what's reported as blue shaded areas in Fig. 18 and 19 of our paper. Certainly one can assume that spectra of blazars in a small energy band (e.g. 1 decade) can be successfully modeled as a power-law).
- Very recently Inoue & Totani (http://adsabs.harvard.edu/abs/2011ApJ...728...73I) who advanced the idea of the blazar sequence being coupled to the X-ray luminosity function published an erratum of their original paper (basically they found a bug in their code). Now their estimate of the contribution of blazars to the background comes to within ~2% (!!) of what we have published.

Why Use The Profile Energy for the LAT Line Search?

- P6V3 FT1 energy is not well suited to perform a line search.
  - ✓ FT1 energy has a number of structures at the few percent level that could be mistaken for photon lines from 5 GeV – 300 GeV. Impacts ULs.
- These structures don't affect typical astrophysical analyses.
- The Energy measurement problem is corrected in Pass7, which will be released this year (2011).

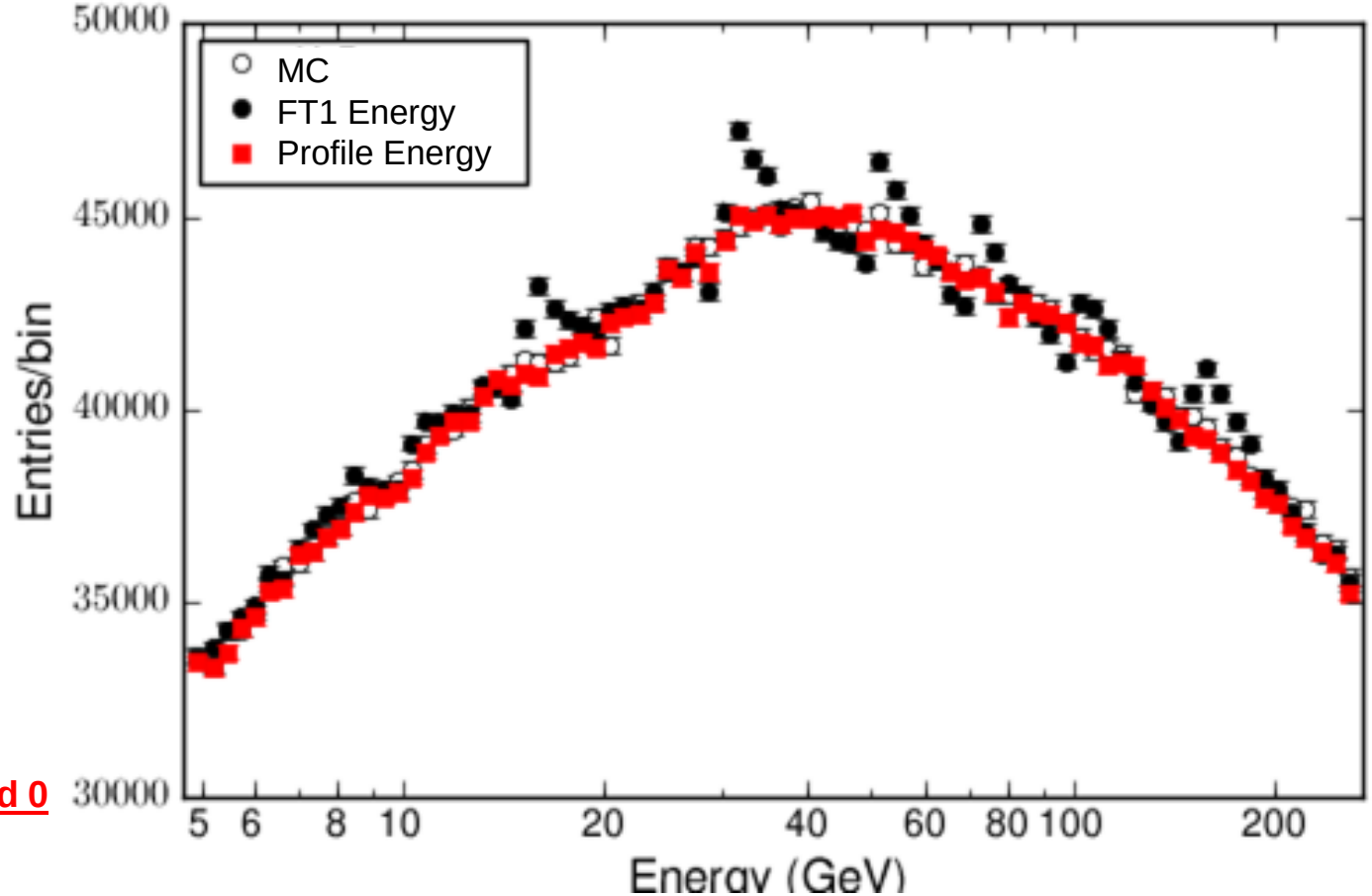

Suppressed 0

Examples of Profile Energy Line Energy Resolution Used for S(E) in Fit.

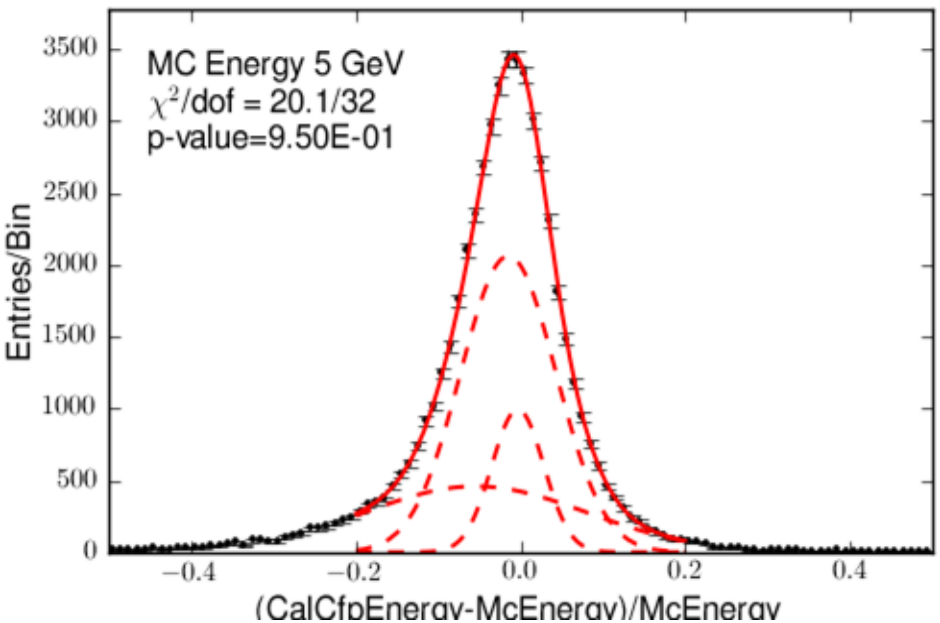

3-Gaussian Fits to MC

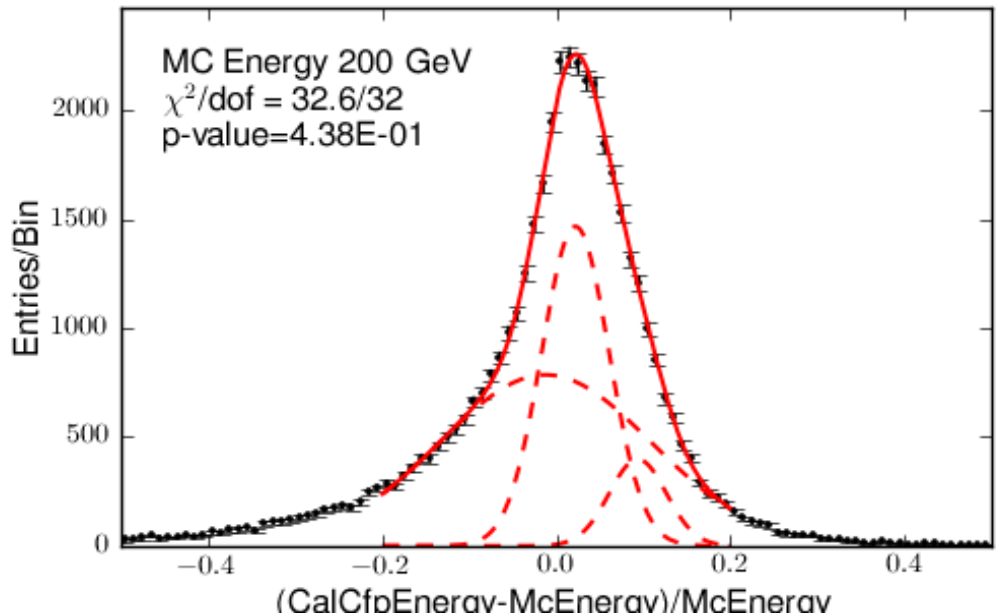

Energy Ranges for Fitting Line limits

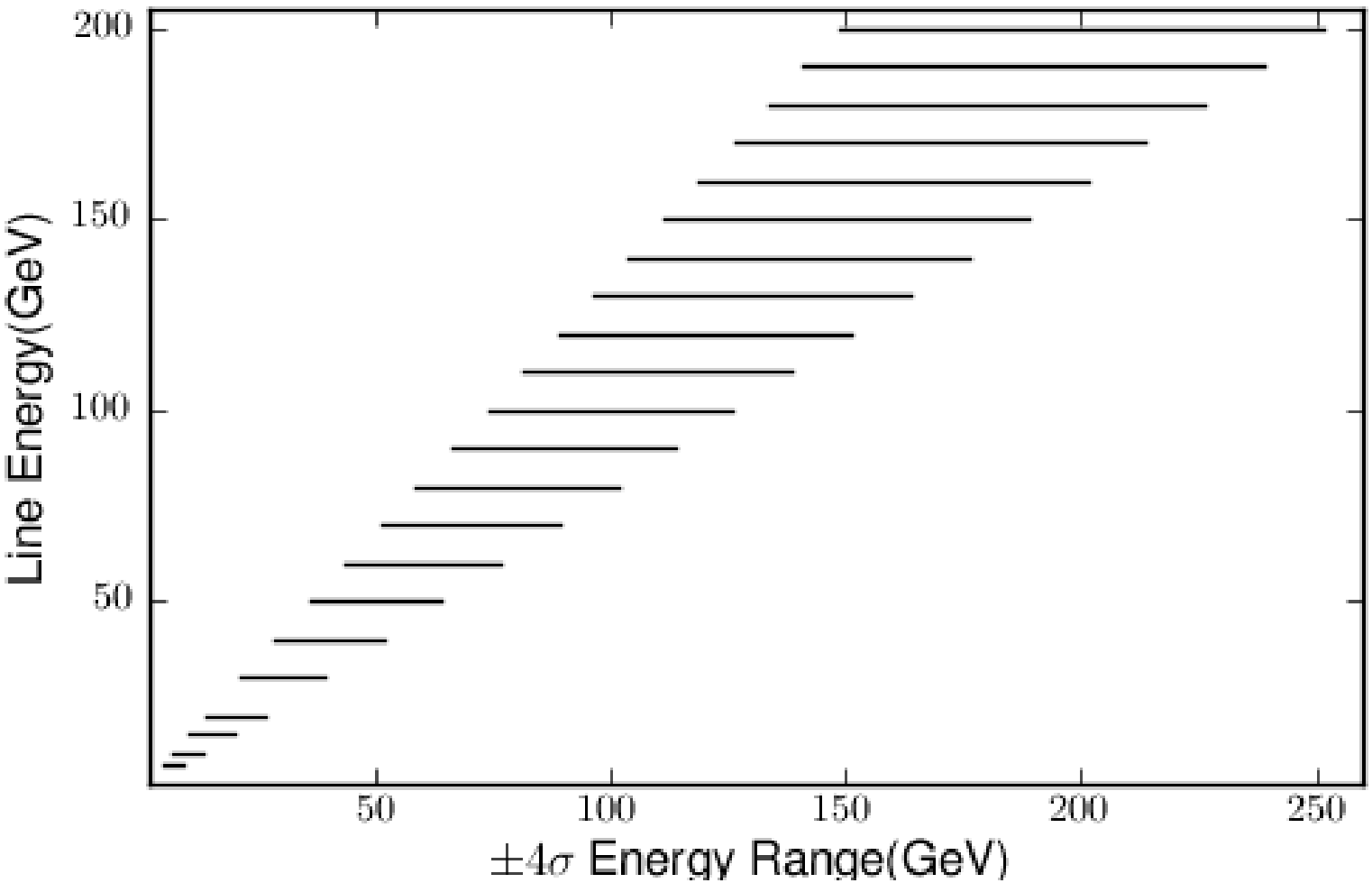

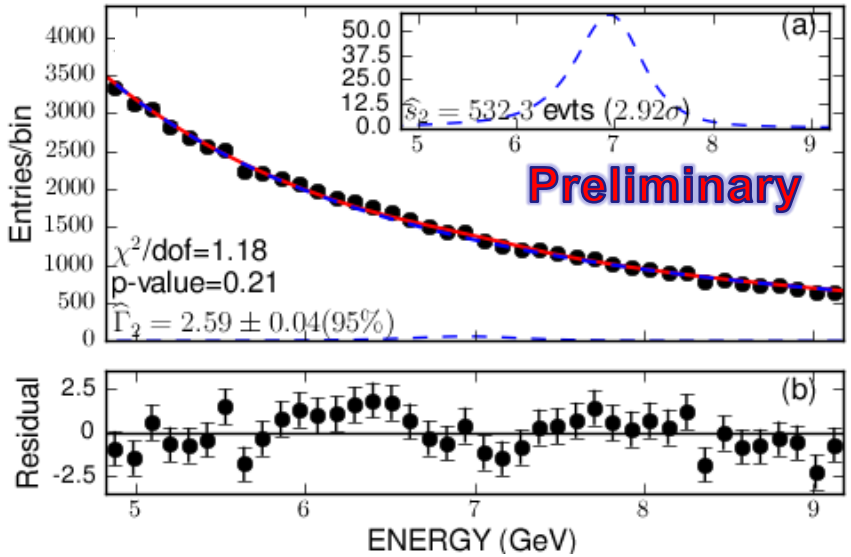

- Using standard event selection we see ~ 3 σ bump at 7 GeV.
- Using standard event selection below 13.2 GeV we estimate a systematic on spectral structures with LAT resolution for E< 13.2 GeV of s/b~3% by not only considering this ROI, but also the control region.

7 GeV signal fitting range (bin center is 7 GeV.)

Remove "CTBCORE" Cut below 13.2 GeV, i.e. for 7 GeV (and 10) GeV fits.

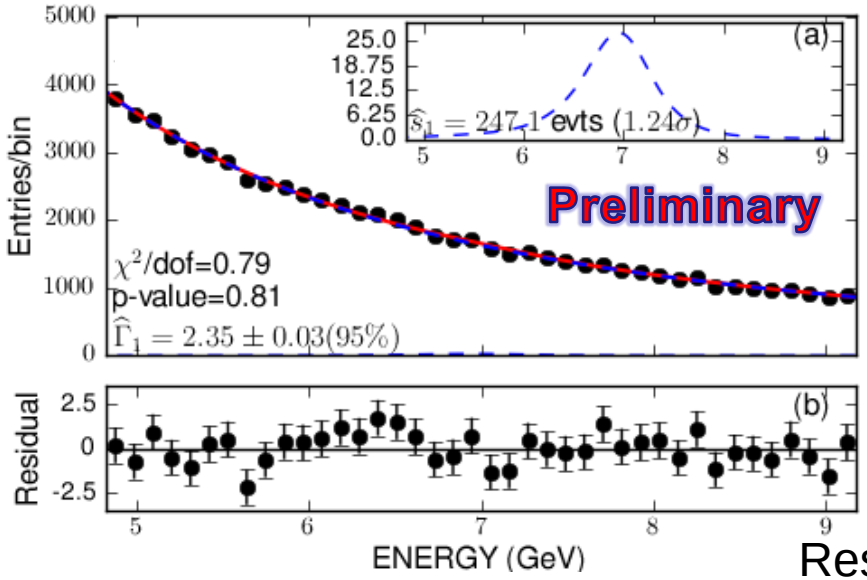

- Removing "CTBCORE" cut we see 1.2 σ bump at 7 GeV.
- Removing "CTBCORE" cut below 13.2 GeV we estimate a systematic on spectral structures with LAT resolution for E< 13.2 GeV of s/b~1%.

Residual = (#counts – model counts)/ √(#counts)

Bobby Samir Acharya, Gordon Kane, Eric Kuflik, Ran Lu, (2011) arXiv:1102.0556v1 [hep-ph]

We consider a solution to the mu-problem within M theory on a G2-manifold. Our study is based upon the discrete symmetry proposed by Witten that forbids the mu-term and solves the doublet-triplet splitting problem. We point out that the symmetry must be broken by moduli stabilization, describing in detail how this can occur. The mu-term is generated via Kahler interactions after strong dynamics in the hidden sector generate a potential which stabilizes all moduli and breaks supersymmetry with m_{3/2} ~ 20 - 30 TeV. We show that mu is suppressed relative to the gravitino mass, by higher dimensional operators, mu ~ 0.1 m_{3/2} ~ 2-3 TeV. This necessarily gives a Higgsino component to the (mostly Wino) LSP, and a small but non-negligible LSP-nucleon scattering cross-section. The maximum, spin-independent cross-sections are not within reach of the current XENON100 experiment, but are within reach of upcoming runs and upgrades.

"If we insist on a good description of the Pamela data plus consistent compactification including m, EWSB, etc, we find an LSP mass from about 140-155 GeV, and an annihilation cross section 2-3.5 x 10^{-24} cm^3/s. The annihilation to γ-Z ranges from 0.7 to 1.2 x 10^{-26}."

Old PRL Result 11 Months of Data

Phys. Rev. Lett. 104, 091302 (2010)

Search for Spectral Lines

- ☺ Smoking gun signal of dark matter.
- ☹ The line signal is generally suppressed, but enhanced in some models
- The signal is the LAT line response function. The background is modeled by a power-law function and determined by the fit
  ⇒ No astrophysical uncertainties.

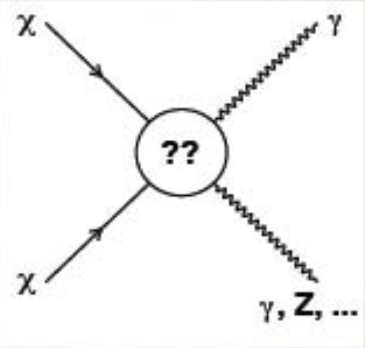

➡ No line detection by Fermi with 11 months of data (30-200 GeV)

Example fit for a 40 GeV line

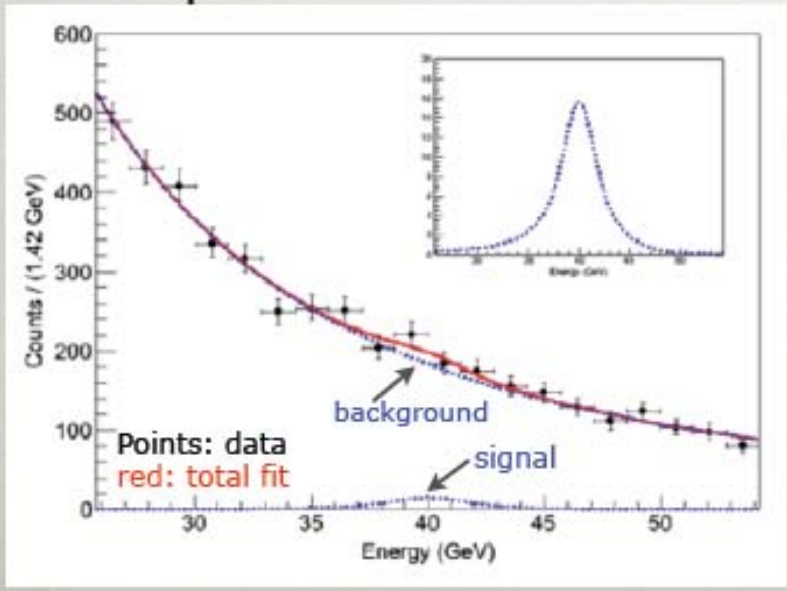

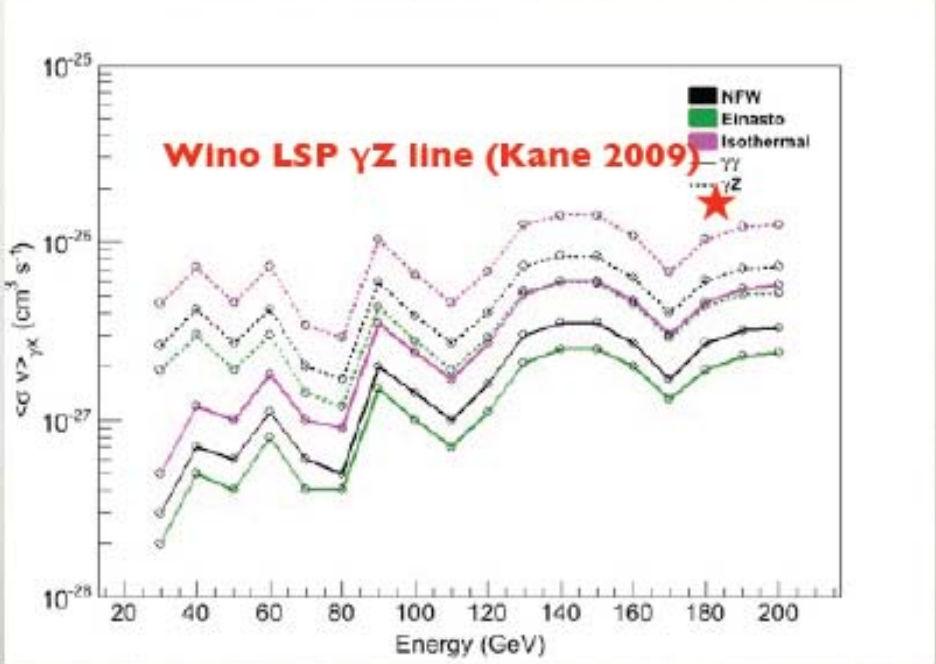

Relating Flux Measurements and Bounds on LED

The following equation relates gamma-ray SED from neutron star $d\Phi/dE$, n, and extra dimensions size R:

distance Extra dimension size (m)

distribution function shown on next slide

$$\boxed{\frac{d\Phi_n}{dE} = k_n \left(\frac{d}{\text{kpc}}\right)^{-2} R^n \frac{dN_n}{dE} \quad [\text{cm}^{-2}\text{s}^{-1}\text{MeV}^{-1}]}$$

$$k_n = \frac{1}{4\pi(3.086\times10^{21}\ \text{cm/kpc})^2}(30\text{MeV})^3 \times (3.17\times10^{-23}\text{MeV}^{-3}\text{s}^{-1})\left(1.52033\times10^{14}\right)^n N_{0,n} \times \frac{2}{3}$$

$\frac{1}{1\times10^9\,\text{yr}\times(100\ \text{MeV})^3}$ decay

$(T/\hbar c)^n$

2 photons per graviton

$$\frac{dN_n}{dE} = \frac{1}{N_{ev}} \frac{dN_n'}{dE}$$

[Initial number of gravitons produced during core collapse]/(RT)^n

$T = 30$ MeV is the progenitor supernova core temperature

Branching ratio BR(2γ)=1/3

Spectrum after attenuation and decay (integral = N_{ev} in case of no attenuation, decay)

N_{ev} = [Number of events simulated]

Table of k_n values

n	k_n
2	6.171E+06
3	5.269E+21
4	4.619E+36
5	4.259E+51
6	4.151E+66
7	4.273E+81

Determining the Distribution of dN/dE_γ

For a given n:

- Sample ω from the distribution: $f(\omega) = \frac{(\omega/T)^{n+2}}{1+\exp(\omega/T)}$
  - Exponential term from detailed balancing
- Sample $\mu = 1/\gamma$ from the function: $G_{n+3}(\mu) = \mu^{n+3}(1-\mu^2)^{1/2}\left(\frac{19}{18}+\frac{11}{9}\mu^2+\frac{2}{9}\mu^4\right)$
  - this is related to the initial distribution of μ from SN core
- The previous two steps determine the mass $m=\mu\omega$ of a simulated graviton in the MC simulation.

- Sample $r(t)$ from the radial distribution, determined by the KK graviton orbital trajectory, a function of μ.
  - Approximate gravitational potential as Newtonian potential for neutron star
  - Radial trajectory for graviton orbits: Harmonic oscillator inside, radial Kepler equation outside
  - Initial condition on β, γ derived from $G_{n+3}(\mu)$.
- Determine the velocity $\beta' c$ as a function of radius from dr/dt
- Photon energy:

$$E_\gamma = \frac{1}{2}\gamma' m(1+\beta'\cos\theta)$$

θ: angle between KK graviton and decay photon

Determining the Spectrum: Accounting for Decay

- Spectra for each source have been corrected for decay

$$\sim \exp\left(-\frac{t_{age}}{\frac{\omega}{m}\tau(m)}\right), \quad \tau(m) = 1\times 10^{9}\,\mathrm{yr}\left(\frac{100\ \mathrm{MeV}}{m}\right)^{3}$$

- Attenuation of signal by decay:
  - Exponential decay: higher mass *h* decay more rapidly
  - Decay to photons, e^+e^-, neutrinos in this mass range
  - Greater effect in older stars

Attenuation in the Magnetosphere

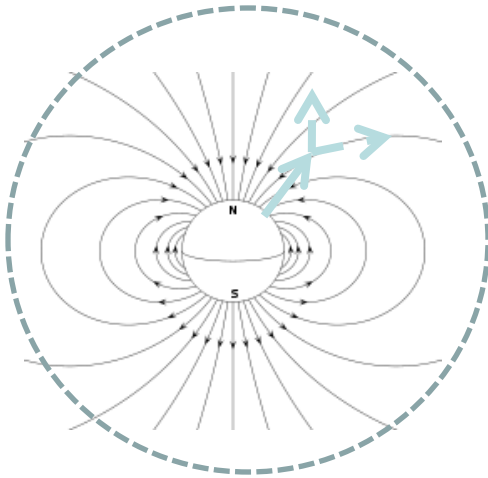

- B-field attenuation :
  - τ_{pp} is the pair production optical depth

$$\sim e^{-\tau_{pp}(E_\gamma, \vec{B}(\vec{r}))}, \quad \tau_{pp}(E_\gamma, \vec{B}(\vec{r})) = \int_{\text{path}} \alpha \, ds$$

  - α is the pair production attenuation coefficient, integrated over the path of photon away from point of decay until $r = 7R_{NS}$ (little change after that).
  - Assume a dipole magnetic field for neutron star, no obliquity nor time dependence
  - Use formulas by Erber, Landau and Lifshitz for pair production
    - Used in models of curvature radiation emission by pulsars
  - Attenuation is a function of χ, related to the product of photon energy and the B-field component perpendicular to photon direction

$$\chi = \frac{E_\gamma}{m_e c^2} \frac{B_\perp}{B_{cr}} \qquad \alpha(\chi) = 0.16 \frac{\alpha_{fs}}{\lambda\!\!\!^{-}_e} \frac{B_\perp}{B_{cr}} \frac{1}{\chi} K^2_{1/3}\left(\frac{2}{3\chi}\right) \qquad B_{cr} = 4.4\text{E}14\ \text{G}$$

Table of Individual Upper Limits (1 year LAT data)

•Flux upper limits (cm^{-2} s^{-1})
•95% confidence level

n	J1856-3754	J0108-1431	J0953+0755	J1136+1551	J0630-2834	J0826+2637
2	5.4E-9	5.9E-9	7.2E-9	5.7E-9	8.1E-9	9.2E-9
3	5.4E-9	5.8E-9	7.5E-9	5.8E-9	9.3E-9	1.1E-8
4	5.5E-9	5.7E-9	8.1E-9	5.9E-9	1.2E-8	1.3E-8
5	5.7E-9	5.7E-9	8.6E-9	6.0E-9	1.4E-8	1.6E-8
6	5.8E-9	5.6E-9	9.3E-9	5.7E-9	1.8E-8	1.9E-4
7	6.1E-9	5.6E-9	1.0E-8	5.9E-9	2.2E-8	2.2E-8

Preliminary

R (m)
95% CL upper limit on compactification radius R.

n	J1856-3754	J0108-1431	J0953+0755	J1136+1551	J0630-2834	J0826+2637
2	1.1E-8	5.8E-8	2.6E-8	2.7E-8	2.8E-8	3.4E-8
3	4.3E-11	1.2E-10	7.5E-11	7.7E-11	8.2E-11	9.2E-11
4	2.8E-12	5.8E-12	4.1E-12	4.2E-11	4.6E-12	5.1E-12
5	5.4E-13	9.7E-13	7.4E-13	7.5E-13	8.5E-13	9.0E-13
6	1.8E-13	3.9E-13	2.4E-13	2.4E-13	2.8E-13	2.9E-13
7	8.6E-14	3.0E-13	1.1E-13	1.1E-13	1.2E-13	1.3E-13

Preliminary